3280–3296 *Nucleic Acids Research, 2017, Vol. 45, No. 6* *Published online 7 February 2017*
doi: 10.1093/nar/gkx071

CNBP acts as a key transcriptional regulator of sustained expression of interleukin-6

Eunhye Lee[1,†], Taeyun A. Lee[1,†], Ji Hyun Kim[2,†], Areum Park[1], Eun A. Ra[1], Sujin Kang[1], Hyun jin Choi[1], Junhee L. Choi[1], Hyunbin D. Huh[1], Ji Eun Lee[2,3,*], Sungwook Lee[4,*] and Boyoun Park[1,*]

[1]Department of Systems Biology, College of Life Science and Biotechnology, Yonsei University, Seoul 03722, South Korea, [2]Department of Health Sciences and Technology, Samsung Advanced Institute for Health Sciences and Technology, Sungkyunkwan University, Seoul 06351, South Korea, [3]Samsung Genome Institute (SGI), Samsung Medical Center, Seoul 06351, South Korea and [4]Cancer Immunology Branch, Research Institute, National Cancer Center, 323 Ilsan-ro, Ilsandong-gu, Goyang-si, Gyeonggi-do 10408, South Korea

Received September 22, 2016; Revised January 23, 2017; Editorial Decision January 25, 2017; Accepted January 26, 2017

ABSTRACT

The transcription of inflammatory genes is an essential step in host defense activation. Here, we show that cellular nucleic acid-binding protein (CNBP) acts as a transcription regulator that is required for activating the innate immune response. We identified specific CNBP-binding motifs present in the promoter region of sustained inflammatory cytokines, thus, directly inducing the expression of target genes. In particular, lipopolysaccharide (LPS) induced *cnbp* expression through an NF-κB-dependent manner and a positive autoregulatory mechanism, which enables prolonged *il-6* gene expression. This event depends strictly on LPS-induced CNBP nuclear translocation through phosphorylation-mediated dimerization. Consequently, *cnbp*-depleted zebrafish are highly susceptible to *Shigella flexneri* infection *in vivo*. Collectively, these observations identify CNBP as a key transcriptional regulator required for activating and maintaining the immune response.

INTRODUCTION

Cellular nucleic acid-binding protein (CNBP), also known as zinc finger protein 9, plays a critical role in forebrain development by regulating cell proliferation and apoptosis during vertebrate organogenesis (1). CNBP has also been proposed to exhibit various biological functions as a nucleic acid chaperone, such as regulating the transcription of *c-myc*, *wnt*, or skeletal muscle chloride channel 1 (*clc1*), and inhibiting the translation of ribosomal protein mRNAs (rp-mRNAs) (2–6). Furthermore, CNBP has been largely implicated in various human diseases, including myotonic dystrophy type 2 (DM2) and sporadic inclusion body myositis (sIBM) (7,8).

Cnbp encodes a 19-kDa protein that contains seven tandem cysteine-cysteine-histidine-cysteine (CCHC) zinc-knuckle repeats, which are composed of 14 amino acids and a glycine/arginine-rich region that is highly similar to the arginine-glycine-glycine (RGG) box of RNA-binding proteins (9). CNBP is a highly conserved protein that shares more than 95% sequence identity among humans, chickens, rats and mice. It is mainly localized to both the nuclei and cytoplasm of cells in mammals, amphibians, chickens and fish (10–14). In particular, several studies have shown that CNBP-mediated DM2 pathogenesis may confer susceptibility to several immune-related diseases, such as rheumatoid arthritis and inflammatory eosinophilic infiltration (15,16). Additionally, hyperactivation of the innate immune response is associated with the pathology of DM (17). In a similar phenomenon, CNBP is correlated with sIBM, which is a type of autoimmune disorder characterized by abnormal inflammatory responses. These responses are caused by an unknown trigger and lead to muscle degeneration and injury (18,19), suggesting that CNBP may directly participate in immune responses.

Cytokines and chemokines are immunoregulatory proteins that act as signaling molecules and control both the innate and adaptive immune response to activate an effective host defense against microbial invaders (20,21). Therefore, its expression must be tightly regulated by transcriptional and post-transcriptional mechanisms during infections, mis-regulated synthesis or turnover of inflammatory

*To whom correspondence should be addressed. Tel: +82 2 2123 5655; Fax: +82 2 312 5657; Email: bypark@yonsei.ac.kr
Correspondence may also be addressed to Ji Eun Lee. Tel: +82 2 3410 6129; Fax: +82 2 3410 0534; Email: jieun.lee@skku.edu
Correspondence may also be addressed to Sungwook Lee. Tel: +82 31 920 2537; Fax: +82 31 920 2542; Email: swlee1905@ncc.re.kr
†These authors contributed equally to the paper as first authors.

cytokines, all of which may exert a pathological effect on chronic inflammation and autoimmunity (22,23). During the stimulation of macrophages with lipopolysaccharide (LPS), which is a surface component of Gram-negative bacteria recognized by Toll-like receptor 4 (TLR4) (24), several transcription factors work together to activate cytokine and chemokine gene expression (25,26). In particular, nuclear factor κB (NF-κB) and interferon regulatory factors (IRFs) are constitutively expressed in various cell types. These factors are induced most rapidly by stimulus-dependent and post-translational modifications, and they are translocated to the nucleus, where they initiate inflammatory gene expression by binding to a specific DNA region on the *cis*-regulatory elements of their target genes (22). After the primary responses, the sequential cascades of transcription factors regulate subsequent gene expression as a positive feed-forward control pathway, which governs the immune system over a prolonged period of time (22,27–28). This regulatory circuit proposes a high degree of complexity in LPS-induced transcriptional regulation, but the gene regulatory network that is involved in the pathogen-evoked inflammatory activation of macrophages is not fully understood.

Here, we describe a previously unknown role for CNBP as a transcription regulator of persistent *il-6* gene expression. Using a DNA–rotein complex pull-down assay, we identified specific CNBP-binding motifs in the promoter regions of sustained cytokines, including interleukin *(il)-1b*, *il-6*, *il-12b*, and *il-15*, and chemokine (C-C motif) ligand 3 *(ccl3)*, *ccl4*, *ccl5*, *ccl7*, *ccl9* and *ccl22*, which are targeted for transcription by CNBP activity. Furthermore, LPS induced *cnbp* expression through a positive autoregulatory mechanism and an NF-κB-dependent manner. We also found that LPS stimulated the translocation of CNBP from the cytosol to the nucleus through a phosphorylation-dependent dimerization mechanism. Consequently, knockdown of *cnbp* in zebrafish showed reduced *il-6* mRNA levels and a greatly decreased number of infiltrating leukocytes into an infected region, thereby leading to severe *Shigella flexneri* infection-induced mortality *in vivo*. Thus, we propose a novel function for CNBP in a regulatory transcriptional circuit for *il-6* mRNA production that involves promotion of the immune response against infection over time.

MATERIALS AND METHODS

Reagents and antibodies

LPS (*Escherichia coli* 026:B6) and 1826 CpG-DNA (5′-TsCsCsAsTsgsAsCsgsTsTsCsCsTsgsAsCsgsTsT-3′) were purchased from Sigma-Aldrich (St Louis, MO, USA) and TIB Molbiol (Berlin, Germany), respectively. DAPI (4′,6-diamidino-2-phenylindole) and actinomycin D were purchased from Sigma-Aldrich. The following antibodies were used: anti-CNBP (ab83038; Abcam, Cambridge, UK or sc-515387; Santa Cruz Biotechnology, Santa Cruz, CA, USA), anti-p65 (sc-8008; Santa Cruz Biotechnology), anti-tubulin (G094; ABM Inc., Richmond, Canada), anti-FLAG (G191; ABM Inc. and M185-3L; MBL International, Woburn, MA, USA), anti-HA (G036; ABM Inc.), anti-Myc (2276; Cell Signaling Technology), anti-GFP (11814460001; Roche, Basel, Switzerland and ab290; Abcam) and anti-Lamin A/C (2032; Cell Signaling Technology).

DNA constructs

Mouse *cnbp* (isoform 1 and 2) and mutants were tagged with hemagglutinin (HA), Myc or green fluorescent protein (GFP) and cloned into retroviral pLHCX or pMSCV vector (Clontech, Mountain View, CA, USA) (HA-CNBP, CNBP-HA, Myc-CNBP, GFP-CNBP, CNBP-HA^{T173A}, CNBP-HA^{T177A} and CNBP-HA$^{T173/177A}$). Mouse complementary DNA encoding p65, TAK1 and CK1 were fused to Myc or Flag and cloned into the retroviral pMSCV vector (Myc-p65, Myc-TAK1 and Flag-CK1). Flag-PKC and Flag-PKA were kindly provided by Dr Young Jun Oh (Yonsei University, South Korea) and Dr Yeun Kyu Jang (Yonsei University), respectively. All GST-fusion constructs were generated by subcloning into the pGEX-6P-1 vector (GE Healthcare, Uppsala, Sweden) (GST-CNBP, GST-HA-CNBP, GST-CNBP Δ1-53, GST-CNBP Δ54-178, GST-CNBP ΔRGG, GST-CNBP ΔNLS, GST-CNBP$^{T173/177A}$ and GST-p65 [356−549]). *Il-6* promoter genes ([−5562 to +49 bp] and [−1624 to +49 bp]), *il-12b* promoter genes (−1062 to +63 bp), and *cnbp* promoter genes (−1444 to +154 bp) were prepared from mouse genomic DNA and cloned into the pGL3 basic vector (Promega, Madison, WI, USA). The deletion mutants of the CNBP-binding site (CTGAAAAA [−1146 to −1139], CTGAAAAA [−518 to −511] and AAATTAGA [−52 to −45]) in the *il-6* promoter region were generated by overlap extension polymer chain reaction (PCR). The shRNA oligonucleotides against CNBP or GFP (control) were annealed and subcloned into the pSUPER retroviral vector (Oligoengine, Seattle, WA, USA). All constructs were verified by sequencing, and all primer sequences are listed in Supplementary Table S1.

Cell culture

Murine RAW 264.7 macrophages (ATCC TIB-71), human embryonic kidney (HEK) 293T cells (ATCC CRL-11268), mouse epithelial fibroblasts (MEFs) and *p65*-deficient MEFs (*p65*$^{-/-}$) were grown in Dulbecco's Modified Eagle Medium (DMEM; HyClone, Logan, UT, USA) containing 10% fetal bovine serum (FBS; HyClone) and penicillin/streptomycin (HyClone). Cells were maintained in an atmosphere of 5% CO_2 in a 37°C humidified incubator. NF-κB *p65*-deficient MEFs were kindly provided by Dr Alexander Hoffmann.

Statistical analysis

All experiments were repeated at least three times with consistent results. Data are presented as means and standard deviations, as noted in the figure legends. Statistical differences between two means were evaluated with the two-tailed, unpaired Student's *t*-test or Mantel-Cox log-rank test. Differences with *P* values less than 0.05 were considered significant. No samples were excluded from the analysis. The data was normally distributed, and the variances were similar between groups. No statistical method was

used to predetermine sample sizes. Instead, sample size determinations were based on previous experiences with experimental variability. The experiments were not randomized, and the investigators were not blinded to allocation during the experiments or the outcome assessments.

RESULTS

CNBP binds to the promoter region of sustained cytokine genes and affects their expression

CNBP has been shown to bind to nucleic acids and regulate the expression of various genes that are involved in forebrain development and proliferation. As described previously, it has also been implicated in immune disorders (1,15–19). Therefore, we investigated whether CNBP may act as a transcriptional regulator in the immune response using a DNA–protein complex pull-down assay. This technique is used to identify specific binding targets and DNA-binding sequences for transcription regulators (29), and thus allowed us to discover new targets of CNBP in the transcriptional regulation of the immune response in macrophages. DNA libraries from the DNA pull-down samples were constructed and sequenced; the sequenced fragments were mapped to the UCSC mm10 genome sequence (Supplementary Figure S1A). As reported previously (30,31), the G-rich consensus sequences occurred with the highest frequency in the targeted regions (Supplementary Figure S1B). Interestingly, sequencing profiles from the DNA-protein pull-down assay demonstrated that CNBP specifically bound to many immune-related genes, including sustained inflammatory genes, and this occurred in 56.6% of total LPS-induced immune-related transcripts (309 genes) (Supplementary Excel file).

To gain insight into the immunological role of CNBP-DNA binding, we focused on the CNBP-mediated regulation of inflammatory gene expression. Notably, the expression of sustained inflammatory genes that were bound to CNBP (e.g. *il-1b, il-6, il-12b, il-15, ccl3, ccl4, ccl5, ccl7, ccl9* and *ccl22*) was severely impaired in *cnbp*-depleted macrophages during LPS stimulation (Supplementary Figure S2A). In contrast, we did not observe any effects on genes that were not bound to CNBP (e.g. tumor necrosis factor-α [*tnf-a*], transforming growth factor-β1 [*tgf- b1*], secreted phosphoprotein 1 [*spp1*], *il-18* and *irf7*) (Supplementary Figure S2A). To determine if the genomic targeting of CNBP occurs by a mechanism involving a nucleic acid chaperone or a transcription factor, we examined whether occupied sites were enriched for specific DNA-binding motifs. We used MEME (32) to find *de novo* consensus motifs that were recognized by CNBP. This analysis revealed two putative sequences of CNBP binding, and these sequences were statistically significant relative to the background frequency (Figure 1A). Strikingly, these motifs were present at the promoter sites of sustained inflammatory genes and also existed in a small window encompassing nucleotides (nt)−4500 to +1 around the transcription start site (TSS) of these genes (Figure 1B). Consistent with the DNA–protein pull-down analysis, a chromatin immunoprecipitation (ChIP) assay with endogenous CNBP antibody showed that LPS induced the binding of CNBP to the promoter regions of *il-1b*, *il-6*, *il-12b*, *il-15, ccl3*, *ccl4*, *ccl5*, *ccl7*, *ccl9*, *ccl22* or *cnbp* (Figure 1C). Collectively, these promoter regions contained a specific sequence corresponding to **A**A(G)A(T)**T**G(T)**AG**A(T) or **CTGAAAA**T(A) (Figure 1B and C). Furthermore, consistent with the RT-PCR results, quantitative reverse transcription-PCR (RT-qPCR) confirmed that the expression of inflammatory genes bound to CNBP, but not of genes were not bound, was severely attenuated by CNBP depletion in LPS-stimulated macrophages (Figure 1D). To exclude the possibility off-target shRNA effects, we used additional shRNAs targeting CNBP (shRNA #2) to examine the effect of CNBP on the expression of its binding or non-binding genes, namely *il-1b*, *il-6* and *tnf-a*. Consistently, CNBP depletion significantly reduced *il-1b* and *il-6* expression, but not *tnf-a* (Supplementary Figure S2B). Therefore, these results suggest that CNBP specifically binds two consensus motifs in the proximal promoter regions of inflammatory genes, which enhances their expression.

CNBP specifically binds to its target genes in a sequence-dependent manner

CNBP binds preferentially to a single-stranded G-rich consensus sequence, and the specific probes containing the 14-nucleotide G-rich sequence or the 5′ UTR sequence from *Xenopus laevis* L4 rp-mRNA (DNA-L4-UTR) have been used to evaluate the binding capability of CNBP (30,31). Therefore, we investigated the possibility that CNBP may bind to single- or double-stranded forms of the specific binding core sequence. We conducted electrophoretic mobility shift assays (EMSA) using recombinant CNBP and a set of biotin-modified probes containing the CNBP-binding consensus motif (Figure 2A). To verify the integrity and quality of purified recombinant CNBP, recombinant proteins were analyzed by sodium dodecyl sulphate-polyacrylamide gel electrophoresis. We clearly observed a band corresponding to the monomer form of GST-CNBP (predicted size, 44 kDa), as well as a band greater than 80 kDa in size in non-reducing conditions, indicating the dimer form of the protein (Supplementary Figure S3A). Prototype DNA probes gave rise to comigrating DNA–protein complexes that contained a recombinant CNBP. As reported previously, CNBP bound to the single-stranded or G-rich probe (Supplementary Figure S3B and C). Markedly, CNBP also bound to a double-stranded sequence with high affinity (Supplementary Figure S3B). To support this result, we determined whether CNBP binds to double-stranded consensus sequences that are present in the promoter regions of inflammatory genes, including *il-1b*, *il-6*, *il-12b*, *ccl4*, *ccl5*, *ccl9* and *cnbp*. We found that CNBP bound to all predicted consensus core sequences with high affinity (Figure 2A, lanes 7–10). The dissociation constant (K_d) values also showed that the binding affinities of the CNBP-binding consensus motifs to GST-CNBP was similar to that of the 26-nt G-rich sequence (Supplementary Figure S3D). Additionally, introducing the HA antibody or unlabeling CNBP-binding double-stranded DNA probes (cold probes) to the EMSA binding reaction blocked GST-HA-CNBP-DNA or GST-CNBP-DNA binding, respectively, indicating that CNBP is capable of binding to the double-stranded consensus sequences (CTGAAAAA or AAATTAGA) (Fig-

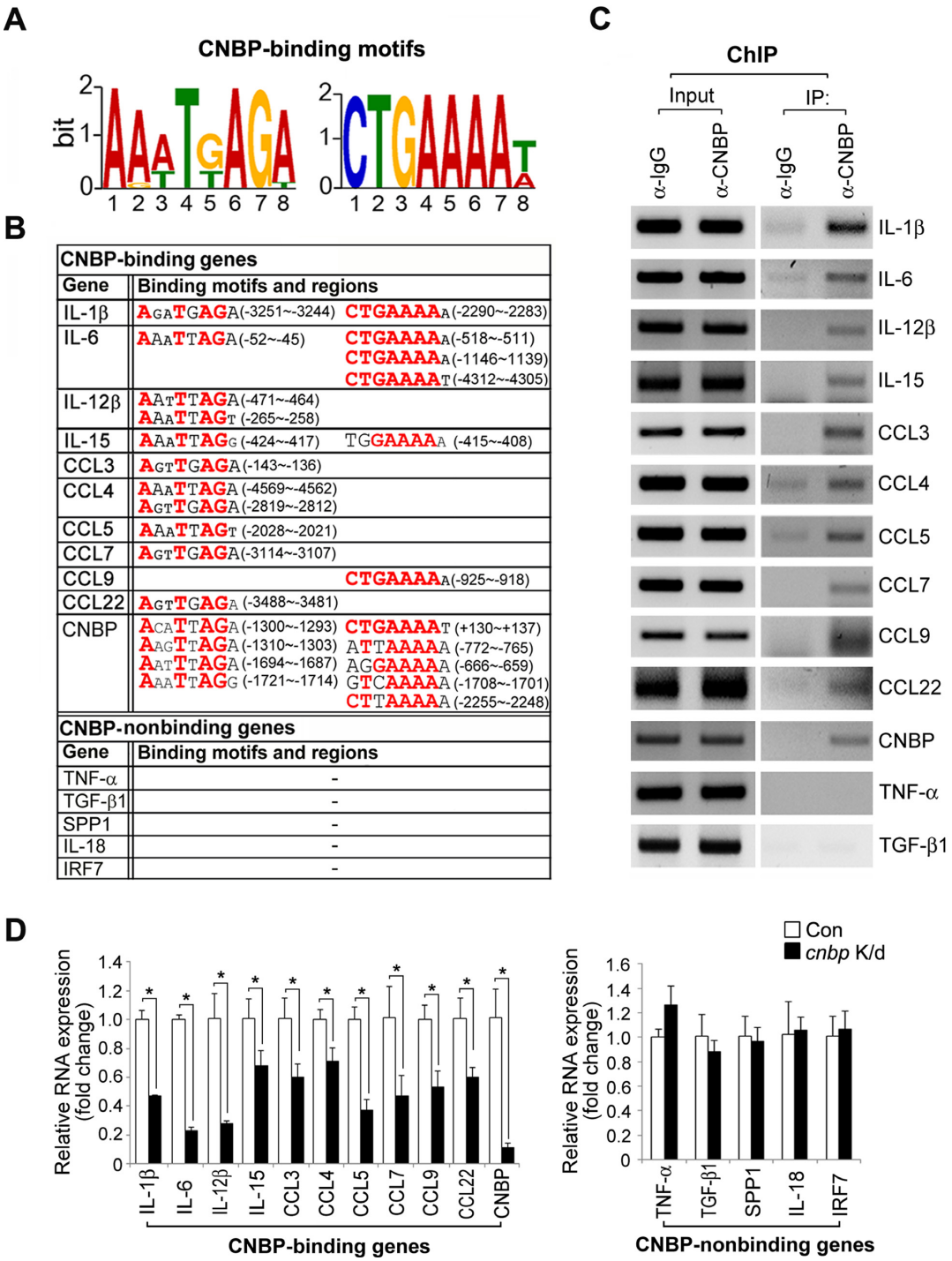

CNBP-binding genes	
Gene	**Binding motifs and regions**
IL-1β	AGATGAGA(-3251~-3244) CTGAAAAA(-2290~-2283)
IL-6	AAATTAGA(-52~-45) CTGAAAAA(-518~-511) CTGAAAAA(-1146~1139) CTGAAAAT(-4312~-4305)
IL-12β	AATTTAGA(-471~-464) AAATTAGT (-265~-258)
IL-15	AAATTAGG(-424~-417) TGGAAAAA (-415~-408)
CCL3	AGTTGAGA(-143~-136)
CCL4	AAATTAGA (-4569~-4562) AGTTGAGA(-2819~-2812)
CCL5	AAATTAGT (-2028~-2021)
CCL7	AGTTGAGA(-3114~-3107)
CCL9	CTGAAAAA(-925~-918)
CCL22	AGTTGAGA (-3488~-3481)
CNBP	ACATTAGA(-1300~-1293) CTGAAAAT (+130~+137) AAGTTAGA(-1310~-1303) ATTAAAAA (-772~-765) AATTTAGA(-1694~-1687) AGGAAAAA (-666~-659) AAATTAGG (-1721~-1714) GTCAAAAA (-1708~-1701) CTTAAAAA (-2255~-2248)

CNBP-nonbinding genes	
Gene	**Binding motifs and regions**
TNF-α	-
TGF-β1	-
SPP1	-
IL-18	-
IRF7	-

Figure 1. CNBP binds to the promoter-proximal regions of sustained cytokines and affects their expression. (**A**) The sequence logo of CNBP-binding motifs, as determined by DNA–protein complex pull-down assay and MEME, is represented. The size of each nucleotide is proportional to the frequency of its appearance at each position. (**B**) Upstream regions of CNBP-binding cytokines have CNBP-binding motifs within 5 kb of the transcription start site (TSS). Bold letters in the consensus sequences indicate highly conserved positions. The numbers in parenthesis refer to CNBP-binding consensus regions in the promoter of indicated genes relative to the TSS. (**C**) CNBP binds directly to sustained cytokine genes. RAW macrophages were treated with LPS (80 ng ml^{-1}) for 2 h, and whole cells were cross-linked with 1% formaldehyde for 10 min. Isolated nuclei were sonicated until the size of the chromatin was below 1 kb. Fragmented chromatin was incubated with anti-CNBP antibody. CNBP-associated promoters were amplified by PCR with the primers indicated in Supplementary Table S2. (**D**) CNBP depletion affects the inflammatory cytokine gene expression. Quantitative real-time RT-PCR analysis of CNBP-binding genes (*cnbp*, interleukin [*il*]-*1b*, *il-6*, *il-12b*, *and il-15*, chemokine ligand 3 [*ccl3*], *ccl4*, *ccl5*, *ccl7*, *ccl9,* and *ccl22*), or CNBP-non-binding genes (tumor necrosis factor [*tnf*]-*a*, transforming growth factor [*tgf*]-*b1*, secreted phosphoprotein 1 [*spp1*], *il-18*, and interferon regulatory factor [*irf7*]), in RAW macrophages transduced with a retrovirus expressing GFP small hairpin RNA (shRNA) (control) or CNBP shRNA after stimulation with LPS (80 ng ml^{-1}) for 12 h. Primer pairs were listed in Supplementary Table S2. *$P < 0.05$ (Student's *t*-test). Data are representative of at least three independent experiments and are presented as mean ± s.d. in D.

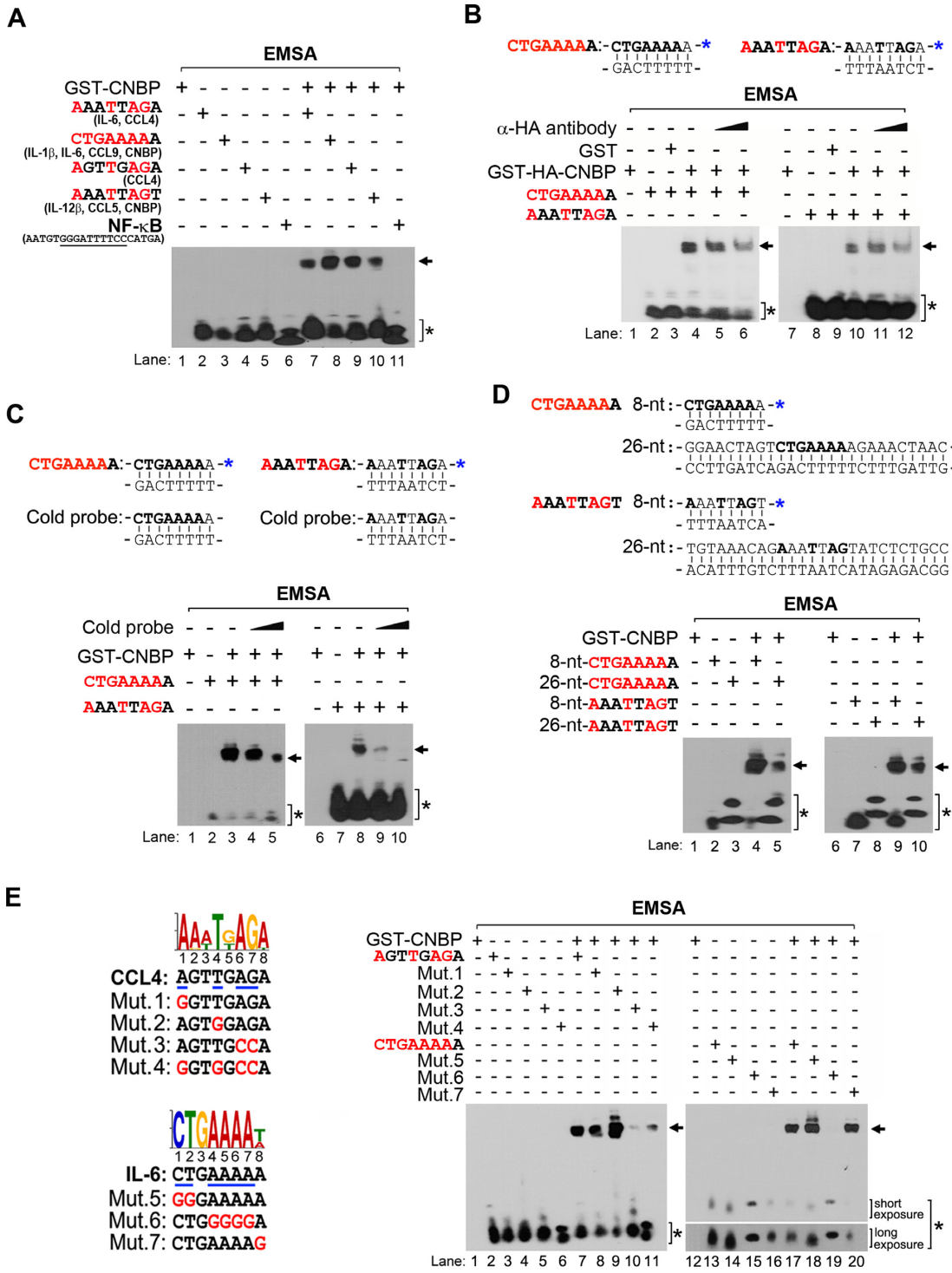

Figure 2. CNBP specifically binds to its target genes in a sequence-dependent manner. (**A**) CNBP binds to the consensus motif-containing probes. EMSA was performed using biotin-labeled dsDNA probes. Recombinant proteins were incubated with the following putative CNBP-binding motifs or nuclear factor (NF)-κB probe: AAATTAGA (*il-6*, *ccl4*), CTGAAAAA (*il-6*, *il-1b*, *ccl9* and *cnbp*), AGTTGAGA (*ccl4*), AAATTAGT (*il-12b*, *ccl5* and *cnbp*), or AATGTGGGATTTTCCCATGA (NF-κB; consensus sequences are underlined). Protein–DNA complexes were resolved on a native polyacrylamide gel. The arrow or asterisk indicates shifted DNA and CNBP complexes or free probes, respectively. The probe was mixed with purified GST-CNBP protein in 1:15 molar ratios. (**B** and **C**) The interaction of CNBP with biotin-labeled double-stranded consensus sequences is masked by antibody-binding or unlabeled dsDNA probes. Purified GST-HA-CNBP or GST-CNBP was pre-incubated with the α-HA antibody or unlabeled dsDNA (cold) probes for 1 h or 15 min before adding the labeled dsDNA probes. The blue asterisks indicate the modification of biotin. (**D**) CNBP binding affinity with target motifs depends on its DNA length. The dsDNA probe was mixed with purified GST-CNBP protein in 1:15 molar ratios. (**E**) The CNBP-target gene interaction occurs in a sequence-specific manner. EMSA for putative CNBP-binding motifs (AGTTGAGA, CTGAAAAA) or mutant probes (Mut. 1–7) using recombinant GST-CNBP. The dsDNA probe was mixed with purified GST-CNBP protein in 1:20 molar ratios. Mutation residues in motifs are indicated with blue lines (wild-type sequences) and red letters (mutation sequences). Data are representative of three independent experiments.

ure 2B, lanes 6 and 12; Figure 2C, lanes 5 and 10). However, it did not bind to NF-κB probes, which do not contain the consensus motif (Figure 2A, lane 11). Moreover, the interaction between CNBP and a long-length probe containing the CNBP-binding consensus sequences was clearly observed, suggesting that CNBP binding to target motifs depends on DNA consensus sequences (Figure 2D, lanes 5 and 10).

Importantly, the mutational analysis of both core consensus sequences showed that mutating the adenine and guanine at positions 6 and 7 of 'AGTTG**AG**A (Mut.3)' or the consecutive four adenines at positions 4–7 of 'CTG**AAAA**A (Mut.6)' resulted in a complete reduction of CNBP-binding activity (Figure 2E, lanes 10 and 19). Additionally, when thymine at the fourth position in an 'AGT**T**GAGA (Mut.2)' motif or cytosine and thymine at the first and second positions in a '**CT**GAAAAA (Mut.5)' motif were with a guanine, which is one of the purines, the binding affinity of CNBP to DNA probes increased over that of wild-type probes (Figure 2E, lanes 9 and 18). Overall, we identified the CNBP-binding elements in the proximal promoter regions of sustained inflammatory genes, and this specific interaction occurs in both single- and double-stranded DNA in sequence-specific and signal-dependent manners.

CNBP directly regulates *il-6* and *il-12b* expression by interacting with the *cis*-regulatory elements

Because previous reports showed that CNBP binds to the G-quadruplex (G4)-forming tandem repeats of G-rich sequences of target genes, thereby leading to transcriptional regulation by rearranging nucleic acid secondary structures (1,30), we first speculated that CNBP may act as a chaperone to regulate its target gene expression. However, in our study, CNBP bound directly to 8-nt consensus sequences, which might be too short to form G4s. Indeed, a *Taq* polymerase stop assay, which is a useful for examining the formation of stable G4 structures *in vitro*, showed no arrest products in the sample containing CNBP and the *il-6* template, unlike G4-forming sequences (Supplementary Figure S4A). These results suggest that, instead of acting as a chaperone, CNBP may function as a transcription factor to activate inflammatory gene promoter and promote its transcription.

In our subsequent studies on the role of CNBP in the transcriptional regulation of inflammatory genes (*il-1b*, *il-6*, *il-12b*, *il-15*, *ccl3*, *ccl4*, *ccl5*, *ccl7*, *ccl9* and *ccl22*) during LPS stimulation, we focused on *il-6* and *il-12b*. These genes possess previously identified TSSs and specifically contain four (*il-6*) and two (*il-12b*) different CNBP-binding consensus sites in their 5′-upstream regions (−4312 to TSS and −471 to TSS, respectively) (Figure 3A). To examine the effect of CNBP on *il-6* or *il-12b* mRNA levels, we measured *il-6* or *il-12b* promoter activity in *cnbp*-depleted and *cnbp*-overexpressed macrophages. After LPS exposure, *cnbp*-depleted and *cnbp*-overexpressed macrophages showed significantly less and more reporter activity than control macrophages, respectively (Figure 3B and C). As noted previously, *il-6* and *il-12b* mRNA levels were significantly impaired by CNBP depletion in LPS-stimulated macrophages (Figure 1D; see also Supplementary Figure S2A), suggesting that CNBP is a positive regulator of *il-6* and *il-12b* expression. This was not due to the CNBP-mediated *il-6* and *il-12b* mRNA stability or the effects of NF-κB activity or its expression levels, which is an initial key transcription factor for *il-6* and *il-12b*, because the transcriptional inhibitor, actinomycin D, had no effect on *il-6* and *il-12b* mRNA levels and no differences in *p65* promoter activity or its expression levels were observed in *cnbp*-depleted cells (Supplementary Figure S4B–D). Moreover, CNBP enhanced *il-6* and *il-12b* promoter activity even in *p65*-deficient cells (Figure 3D), indicating that CNBP is capable of directly regulating *il-6* and *il-12b* mRNA production.

We analyzed the regulatory elements of the *il-6* promoter in detail. Activity of the *il-6* promoter region that encompasses nucleotides −1624 to the TSS, which contains three CNBP-binding motifs, was significantly increased in an LPS-dependent fashion. This result was similar to that of the reporter gene containing the distal region (−5562 to TSS) (Figure 3E), suggesting that the proximal promoter region, rather than distal sites, is required for CNBP-mediated *il-6* expression. To determine which CNBP-binding motif in the *il-6* promoter region is essential for its promoter activity, we removed each consensus motif individually or in combination (Figure 3F). Transactivation of all mutants by CNBP considerably blocked promoter activity, suggesting that each CNBP-binding motif in the proximal promoter region is required for *il-6* expression (Figure 3G). Thus, CNBP directly regulates *il-6* and *il-12b* expression, and CNBP-induced gene transcription depends on a specific consensus sequence that is responsible for CNBP binding.

The RGG domain of CNBP is essential for regulating *il-6* expression

CNBP contains structural features, including seven zinc-knuckle motifs and an RGG box, which is a proposed RNA/DNA-binding motif. To examine if the RGG box is involved in target DNA-binding capability and promoter activities, we generated a construct encoding the first zinc domain and RGG region of CNBP that corresponds to amino acids 1−53 (Δ54−178), along with a deletion mutant lacking either the RGG box (ΔRGG) or the N-terminal region composed of amino acids 54−178 (Δ1−53) (Figure 4A). Similar to wild-type CNBP, the RGG-containing N-terminal (CNBP-1−53) region bound to a double-stranded DNA probe that contained the CNBP-binding sequence (CTGAAAAA) (Figure 4B, lane 8). In contrast, the ΔRGG and Δ1−53 mutants had significantly reduced DNA binding (Figure 4B, lanes 9 and 10). Furthermore, the ΔRGG mutant of CNBP exhibited defects in *il-6* promoter activity (Figure 4C), suggesting that the RGG box of CNBP is indispensable for target DNA binding and promoter activation.

The *cnbp* gene undergoes alternative splicing to encode four splice isoforms in mice. Isoform 1 (Iso1) encodes a full-length CNBP of 178 amino acid residues, which was referred to as 'WT' in this study. The amino acid sequence of isoform 2 (Iso2) is similar to that of isoform 1 except lacking one amino acid (G) at the C-terminal end of the RGG box and six amino acids (FTSDRG) at the N-terminal end

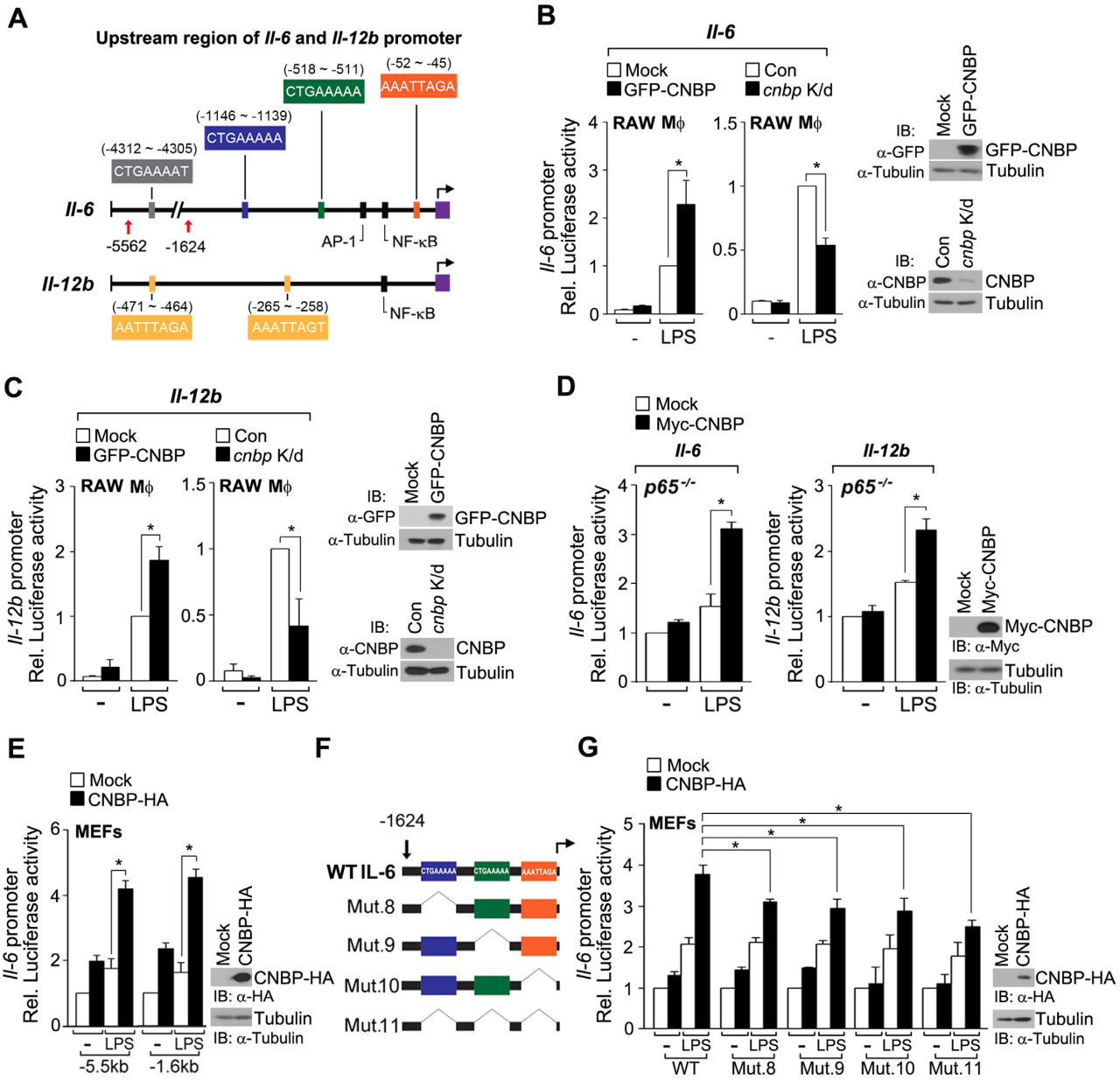

Figure 3. CNBP directly regulates *il-6* and *il-12b* expression by interacting with the *cis*-regulatory elements. (**A**) Schematic representation of the upstream region of *il-6* and *il-12b* in mice. The putative CNBP-binding sequences were located in the *il-6* or *il-12b* promoter. Black boxes indicate the consensus sites for AP-1 and NF-κB in the *il-6* promoter and NF-κB in the *il-12b* promoter. The transcriptional start site is marked by the violet box. (**B** and **C**) CNBP activates *il-6* and *il-12b* expression. Luciferase assays of *il-6* and *il-12b* promoter activity in RAW macrophages expressed an empty vector or GFP-CNBP (left) and GFP shRNA or CNBP shRNA (right). Cells were then transfected with the *il-6* or *il-12b* luciferase reporters and the *Renilla* reporter after stimulation with LPS (80 ng ml^{-1}) for 12 h. *$P < 0.05$ (Student's *t*-test). (**D**) CNBP enhances *il-6* or *il-12b* promoter activity in *p65*-deficient cells. Luciferase assays of *il-6* and *il-12b* promoter activity in *p65*$^{-/-}$ MEFs transfected with Myc-CNBP and the *Renilla* reporter, along with the *il-6* or *il-12b* luciferase reporter. MEFs were then incubated with LPS (80 ng ml^{-1}) for 12 h. *$P < 0.01$ (Student's *t*-test). (**E**) The proximal promoter region of *il-6* is required for CNBP-mediated mRNA production. Luciferase assay of *il-6* promoter activity in MEFs transfected with an empty vector (mock) or CNBP-HA vector, and then incubated with LPS (80 ng ml^{-1}) for 12 h. *$P < 0.01$ (Student's *t*-test). (**F**) Schematic presentation of wild-type (WT) or deletion mutants of the *il-6* promoter [−1624 to +49]. Mutations 8, 9 or 10 (Mut. 8, 9, 10) represents deletions of CTGAAAAA [−1146 to −1139], CTGAAAAA [−518 to −511] or AAATTAGA [−52 to −45], respectively. All three putative CNBP-binding are deleted in mutation 11 (Mut. 11). (**G**) The CNBP-binding motif in the proximal promoter region is required for *il-6* expression. MEFs were transfected with an empty vector (mock) or WT CNBP-HA vector, along with the *Renilla* reporter and the WT *il-6* luciferase reporter or its mutants (Mut. 8, 9, 10 or 11). Cells were stimulated with LPS (80 ng ml^{-1}) for 12 h. *$P < 0.01$ (Student's *t*-test). Immunoblot analysis of CNBP expression levels (right panels of B, C, D, E and G). Data are representative of at least three independent experiments and are presented as mean ± s.d. in B, C, D, E and G.

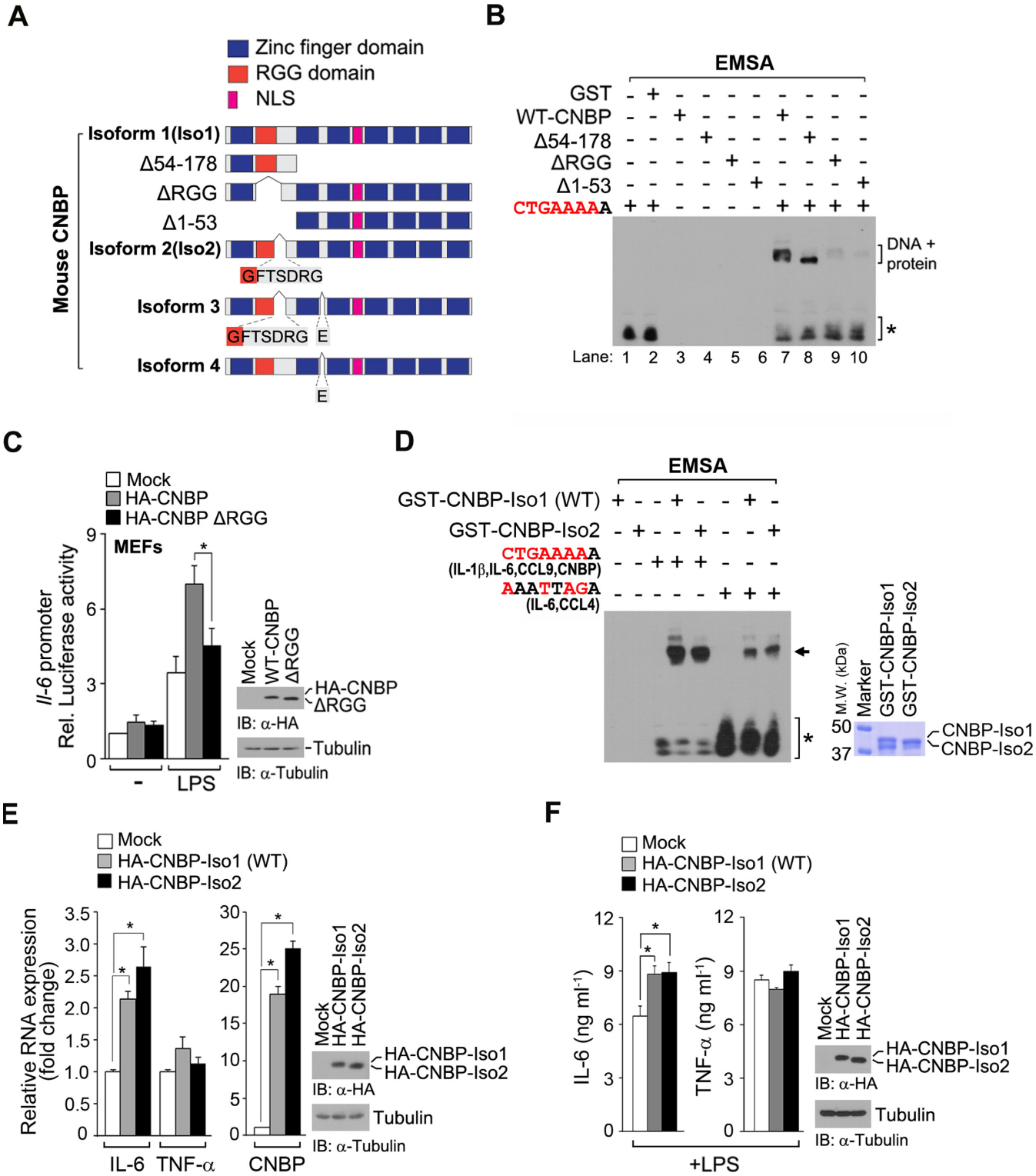

Figure 4. The RGG domain of CNBP is essential for regulating *il-6* expression. (**A**) Domain mapping of CNBP, deletion mutants ([Δ1−53], [Δ54−178] and [ΔRGG]), or its isoforms. CNBP possesses NLS (nuclear localization signal), RGG and zinc finger domains. (**B**) The RGG box of CNBP is important for target DNA binding. Wild-type CNBP and mutant CNBP with GST tags ([WT-CNBP], [Δ54−178], [ΔRGG] and [Δ1−53]) were purified. Recombinant proteins were incubated with the CNBP-binding motif (CTGAAAAA), and protein–DNA complexes were resolved on a native polyacrylamide gel. Oligonucleotides were labeled with biotin. GST was used as a negative control. The dsDNA probe was mixed with purified GST-CNBP protein in 1:15 molar ratios. (**C**) The RGG box of CNBP is required for target gene promoter activation. MEFs were transfected with an empty vector (mock), WT HA-CNBP vector or HA-CNBP (ΔRGG) vector, along with the *il-6* luciferase reporter and *Renilla* reporter and then stimulated with LPS (80 ng ml^{-1}) for 12 h. Luciferase activity was measured and normalized to *Renilla* luciferase activity. *$P < 0.01$ (Student's *t*-test). (**D–F**) Effect of CNBP isoform 1 or 2 on the ability of target-gene binding or IL-6 expression. *$P < 0.01$ (Student's *t*-test) in E or *$P < 0.05$ (Student's *t*-test) in F. Immunoblot analysis or coomassie blue staining of CNBP expression (right panels of C–F). Data are representative of at least three independent experiments and are presented as means ± s.d. in C, E and F.

of the linker region between the first and second zinc finger. Isoforms 3 and 4 are the same as isoforms 2 and 1, respectively, with the exception of a sequence change where one amino acid is deleted (Figure 4A). Because the RGG box of CNBP is indispensable for target DNA binding, we focused on CNBP isoform 2 (CNBP-Iso2). Although the binding affinities of the two consensus 8-nt sequences to CNBP-Iso2 were slightly less than the binding affinity to CNBP-Iso1, CNBP-Iso2 was clearly capable of binding CNBP-binding consensus sequences and activating IL-6 expression, but not TNF-α expression, in a pattern similar to that of full-length CNBP (Figure 4D–F). This indicates that the glycine residue positioned in the last position of RGG box is not involved in CNBP-mediated *il-6* expression. Taken together, we conclude that the entire sequence of the CNBP RGG region is required for facilitating *il-6* expression.

Cnbp expression is induced by NF-κB activation and positive autoregulation

DNA–protein complex pull-down analysis revealed the existence of 13 CNBP-binding sequences with a high coverage read on their own proximal promoter regions (Figure 1B). To assess whether this interaction changes over time after LPS stimulation, we examined the kinetics of these binding events in LPS-stimulated macrophages. CNBP bound to its own promoter after 1 h of LPS stimulation, and its binding remained constant throughout the 12 h exposure (Figure 5A). In addition, the binding of CNBP to the *cnbp* promoter was detected after 1 h and exhibited significant increases at 2 and 6 h, which is similar to that of CNBP binding to the *il-6* promoter (Figure 5A). Consistently, no interaction of CNBP with the *tnf-a* or *tgf-b1* promoter was observed. These findings indicate a temporal characteristic of CNBP activation and suggested that CNBP may function in subsequent waves of target gene induction during LPS stimulation. Next, we hypothesized that LPS-mediated NF-κB activation may affect *cnbp* expression. Interestingly, the *cnbp* promoter region is enriched with unique binding motifs for NF-κB (Supplementary Figure S5A). Notably, the ChIP assay showed that NF-κB-p65 bound to the *cnbp* promoter, and its interaction was observed after 30 min, peaked at 1 h, and gradually decreased 2 h after LPS stimulation (Figure 5B). A similar pattern was observed for NF-κB-p65 interacting with the *il-6, tnf-a* promoter, but not *tgf-b1* (Figure 5B). These results suggest that NF-κB-p65 binding events occur rapidly in response to LPS, and the recruitment of CNBP to the *il-6* promoter or its own promoter occurs later.

Next, we determined if *cnbp* transcription is induced by CNBP and NF-κB-p65 interactions with the promoter. Luciferase reporter activity from the *cnbp* promoter was affected by NF-κB and CNBP, and CNBP mRNA or protein levels significantly increased in LPS-stimulated cells (Figure 5C; see also Supplementary Figure S5B and C). We also clearly observed that *cnbp* expression was impaired in *p65*-deficient MEFs (Figure 5D). The expression of *cnbp* was not induced in *p65*-deficient MEF cells at 1 h after LPS stimulation; however, a significant increase in *cnbp* expression was observed at 6 or 12 h (Figure 5D). These results suggest that NF-κB acts as the initial activator of *cnbp* transcription, and CNBP binds to its own promoter to obtain transcriptional activation at later time points.

Because *il-6* expression is regulated by a major transcription factor (NF-κB), we further characterized the regulatory network between CNBP and NF-κB with regard to *il-6* expression. As reported previously (26), ChIP analysis revealed that NF-κB-p65 bound to the *il-6* promoter within 30 min after LPS stimulation (Figure 5B). Consistently, NF-κB and IRF dissociate from target promoters and are exported from the nucleus at 1 h after LPS stimulation, terminating activation (22,26,33–34). Interestingly, the expression of 'sustained cytokines' (e.g. *ccl3*, *ccl4*, *ccl5*, *ccl9*, *il-1b* and *il-6*) (25), which we identified as CNBP-binding genes, increased steadily at the early time points after LPS induction and eventually plateaued over the later time points, when the interaction of CNBP with the *il-6* or its own promoter clearly occurred. Based on previous reports and our results, we hypothesized that *il-6* expression may require coordinated, temporal control of NF-κB and CNBP. To confirm this possibility, we examined the effects of CNBP depletion or overexpression on *il-6* expression during prolonged LPS stimulation. In *cnbp*-depleted macrophages, persistent induction of *il-6* transcription through 6 h of LPS treatment was severely impaired (>9-fold change) (Figure 5E). We also observed that the induction of short-term *il-6* transcription (1 h) after LPS stimulation decreased in *cnbp*-depleted macrophages, but this decrease was lower than that of the late responses (6 h) (Figure 5E). In contrast, *cnbp*-overexpressing macrophages exhibited a large increase in *il-6* expression after 6 h of LPS stimulation. Similar to CNBP depletion, the induction of short-term *il-6* expression after LPS stimulation was slightly increased in *cnbp*-overexpressing macrophages relative to wild-type cells (Figure 5E). Moreover, *il-6* expression was clearly observed even in *p65*-deficient cells at 6 h after LPS stimulation. Furthermore, *cnbp*-overexpressing cells produced large amounts of *il-6* transcript (Figure 5F). Collectively, LPS activates NF-κB, which binds directly to the promoters of *il-6* and *cnbp* to activate moderate amounts of their production quickly. Subsequently, increased levels of CNBP activate its own transcription via autoregulation, enabling prolonged, direct expression of *il-6*, thereby leading to the sustained production of IL-6 during persistent LPS stimulation.

LPS induces the translocation of CNBP to the nucleus by specific kinase-dependent phosphorylation and phosphorylation-mediated dimerization

Because pathogenic infections stimulate the translocation of transcription factors to the nucleus where they activate expression of the immune-related genes, we explored the subcellular localization of CNBP in primary bone marrow-derived macrophages (BMDMs) after LPS stimulation. CNBP resided mostly in the cytosol of unstimulated macrophages, but translocated to the nucleus upon LPS stimulation (Figure 6A). To confirm the nuclear targeting of CNBP in response to LPS, we separated protein lysates into cytosolic and nuclear fractions. CNBP was unambiguously detected in the nuclear fraction, which was consistent with the results from the immunofluorescence assay (Figure 6B, lane 6). Markedly, deletion of the putative nuclear

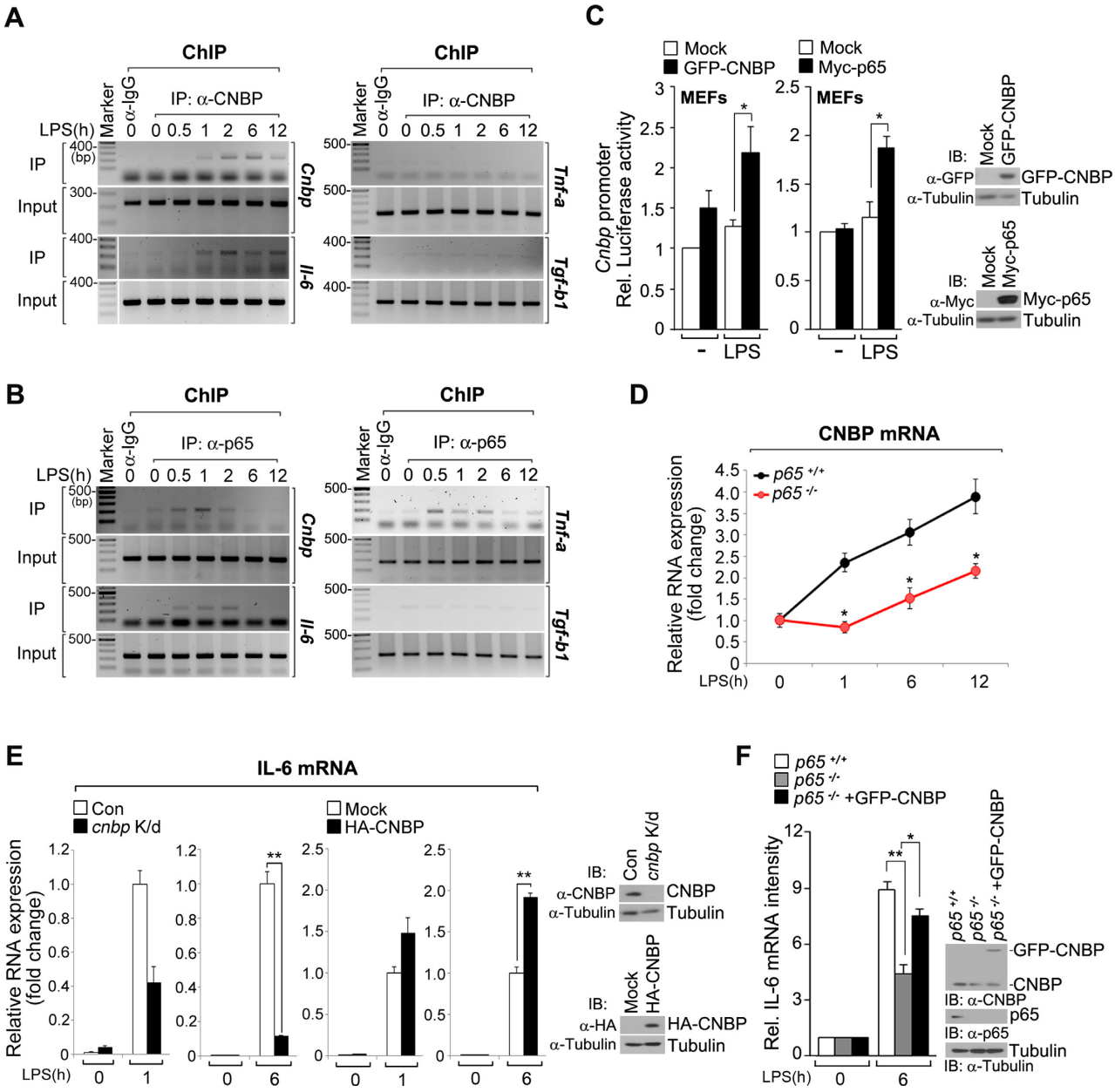

Figure 5. Transcriptional regulatory circuit involving CNBP, NF-κB, and IL-6. (**A**) CNBP binds to *il-6* and its own promoter after 1 h of LPS stimulation. ChIP analysis in RAW macrophages after stimulation with LPS (80 ng ml^{-1}) for 0, 0.5, 1, 2, 6 or 12 h. Eluted chromatin was used for PCR analysis of the *cnbp*, *il-6*, *tnf-a* and *tgf-b1* promoter regions. Input, DNA without immunoprecipitation. (**B**) NF-κB subunit p65 binds rapidly to the promoters of *cnbp*, *il-6* and *tnf-a* after LPS stimulation. RAW macrophages were stimulated with LPS (80 ng ml^{-1}) for the indicated times, and ChIP analysis was performed using the anti-p65 or anti-mouse IgG antibodies. (**C**) *Cnbp* promoter activity is dependent on NF-κB and CNBP. Luciferase assay of CNBP activity in MEFs transfected with an empty vector (mock) or GFP-CNBP (left) and Myc-p65 (right) after stimulation with LPS (80 ng ml^{-1}) for 12 h. *$P < 0.01$ (Student's *t*-test). (**D**) RT-qPCR analysis of *cnbp* in WT or *p65*$^{-/-}$ MEFs after treatment with LPS (80 ng ml^{-1}) for 0, 1, 6 or 12 h. *$P < 0.01$ (Student's *t*-test). (**E**) The effect of CNBP depletion or overexpression on the sustained expression of *il-6*. RT-qPCR analysis of *il-6* mRNA transcripts in WT, *cnbp*-depleted (K/d) or HA-CNBP-overexpressing macrophages stimulated with LPS (80 ng ml^{-1}) for the indicated times, normalized to the amount of *gapdh*. **$P <$ 0.01 (Student's *t*-test). (**F**) Amount of *il-6* mRNA expression in WT and *p65*-deficient MEFs expressing either mock or GFP-CNBP proteins, stimulated with LPS (80 ng ml^{-1}) for the indicated times. Expression was quantified by densitometry of bands and reported relative to *gapdh*. Densitometry of mRNA bands were quantified by three independent experiments. *$P < 0.05$ and **$P < 0.01$ (Student's *t*-test). Immunoblot analysis of CNBP or p65 expression levels (right panels of C, E and F). Data are representative of three independent experiments and are presented as mean ± s.d. in C, D, E and F.

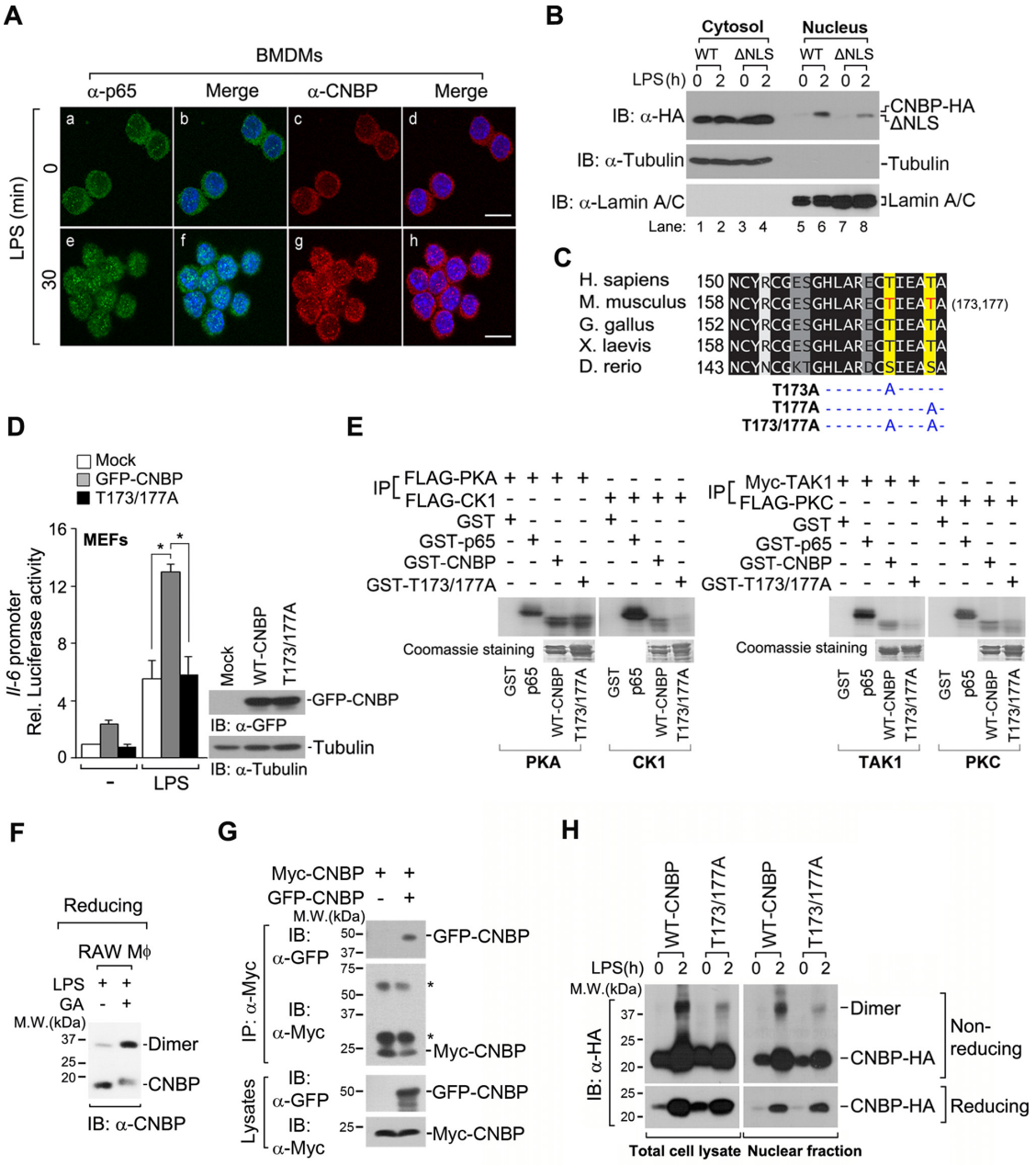

Figure 6. LPS induces the translocation of CNBP to the nucleus by phosphorylation-mediated dimerization. (**A**) CNBP translocates to the nucleus from the cytosol in LPS-stimulated macrophages. Confocal microscopy of bone marrow-derived macrophages (BMDMs) that were stimulated with 80 ng ml^{-1} LPS for 0 or 30 min and then stained with DAPI and immunolabeled with anti-p65 antibody or anti-CNBP antibody. Scale bar, 5 μm. (**B**) The NLS of CNBP is important for the targeting of CNBP to the nucleus in response to LPS. Immunoblot analysis of CNBP or CNBP mutant (ΔNLS) in cytosolic and nuclear fractions of RAW macrophages after treatment with LPS (80 ng ml^{-1}) for 0 or 2 h. Tubulin and lamin A/C were analyzed as loading controls for cytosolic and nuclear fractions, respectively. (**C**) C-terminal region of CNBP was aligned, and the conservation of residues is highlighted in shades of gray. Darker colors represent more conserved residues. Residues highlighted are Thr^{173} and Thr^{177} in the mouse. T173A, T177A and T173/177A indicate the point mutation at Thr^{173}, Thr^{177} and Thr^{173}/Thr^{177} to alanine of CNBP. (**D**) Both putative phosphorylation sites (Thr^{173} and Thr^{177}) are required for the transcriptional activity of *il-6* in response to LPS. MEFs were transfected with an empty vector (mock), wild-type GFP-CNBP vector or GFP-CNBP$^{T173/177A}$ vector, along with the *il-6* luciferase reporter and *Renilla* reporter. Cells were then stimulated with LPS (80 ng ml^{-1}) for 12 h. *$P < 0.05$ (Student's *t*-test). Immunoblot analysis of wild-type GFP-CNBP or GFP-CNBP$^{T173/177A}$ protein expression (right). (**E**) PKC, CK1 or TAK1 is responsible for LPS-mediated CNBP phosphorylation. HEK 293T cells were transfected with FLAG-PKA, FLAG-CK1, Myc-TAK1 or FLAG-PKC, and cell lysates were immunoprecipitated with anti-FLAG or anti-Myc antibodies. Phosphorylated CNBP was resolved by sodium dodecyl sulphate-polyacrylamide gel electrophoresis and analyzed by autoradiography. Coomassie blue stained gels are shown in bottom panels. GST was used as a negative control. (**F**) Dimerization of endogenous CNBP is induced by LPS stimulation. RAW macrophages were treated with LPS (80 ng ml^{-1}) for 2 h. GA, glutaraldehyde. (**G**) The formation of CNBP dimers was determined by co-immunoprecipitation (Co-IP). IP of Myc-CNBP from HEK 293T cells transfected with Myc-CNBP and GFP-CNBP, followed by immunoblot analysis (IB) with antibody to Myc or GFP. Asterisks indicate the IgG heavy and light chains. (**H**) The phosphorylation of CNBP is critical for its dimerization. The dimer forms of the total cell lysates (left) or nuclear fraction (right) of CNBP-HA were detected by immunoblot analysis under non-reducing conditions after treatment with LPS (80 ng ml^{-1}) for 2 h. Data are representative of three independent experiments and are presented as mean ± s.d. in D.

translocation signal CNBP (ΔNLS) exhibited a decrease in LPS-mediated nuclear targeting when compared with wild-type CNBP (Figure 6B, lanes 6 and 8). These results suggest that the NLS of CNBP is important for the targeting of CNBP to the nucleus in response to LPS.

The phosphorylation of master transcription factors is a critical step in nuclear translocation, innate immune response induction and cytokine production. Particularly, zebrafish CNBP is phosphorylated by cAMP-dependent protein kinase (PKA), and this phosphorylation occurs on serine (Ser) 158 (35). Therefore, we hypothesized that LPS may induce CNBP phosphorylation and result in nuclear targeting. Although a serine residue (Ser^{158}) is found in zebrafish, the threonine (Thr) residue is highly conserved in all known vertebrate sequences at equivalent positions (35) (Figure 6C). We performed site-directed mutagenesis of CNBP to replace Thr^{173}, Thr^{177} or both Thr residues with an alanine residue(s), thus generating $CNBP^{T173A}$, $CNBP^{T177A}$ or $CNBP^{T173/177A}$, respectively (Figure 6C). No statistically significant inhibition of *il-6* promoter activity was observed when single-point mutants ($CNBP^{T173A}$ or $CNBP^{T177A}$) were analyzed (Supplementary Figure S6A). Under LPS stimulation, the double-point mutant ($CNBP^{T173/177A}$) showed greatly reduced promoter activity of *il-6* when compared with wild-type CNBP (Figure 6D). This suggests that both putative phosphorylation sites (Thr^{173} and Thr^{177}) are required for the transcriptional activity of *il-6* in response to LPS.

To evaluate whether CNBP phosphorylation occurs on Thr^{173} and Thr^{177}, we conducted an *in vitro* kinase assay involving PKA, which is known to phosphorylate zebrafish CNBP. PKA was involved in the phosphorylation of mouse CNBP, but Thr^{173} and Thr^{177} were not direct substrates for PKA, as there was no significant difference in phosphorylation between wild-type CNBP and $CNBP^{T173/177A}$ (Figure 6E). Therefore, we used a phosphorylation prediction algorithm to identify putative kinases that are capable of CNBP phosphorylation. Casein kinase 1 (CK1), tat-associated kinase 1 (TAK1) and protein kinase C (PKC) were identified as putative kinases for phosphorylating $CNBP^{T173/177A}$ (Supplementary Figure S6B). As previously reported (36–38), PKA, CK1 and PKC kinases are involved in NF-κB phosphorylation (Figure 6E). Notably, CNBP was effectively phosphorylated by all predicted kinases, and the phosphorylation of the $CNBP^{T173/177A}$ was dramatically inhibited (Figure 6E). These results demonstrate that CK1, TAK1 or PKC is responsible for CNBP phosphorylation at Thr^{173} and Thr^{177}.

In many transcription factors, such as IRF3, signal-dependent phosphorylation of the IRF3 serine cluster is essential for its dimerization. The cluster subsequently enters the nucleus, where it works with NF-κB to turn on type I interferons and other cytokines (39). Thus, we examined whether CNBP phosphorylation induces its dimerization and subsequent translocation to the nucleus to activate target genes. Under non-reducing gel conditions, we observed the appearance of a protein of 35∼38 kDa, corresponding to the predicted molecular weight of CNBP dimers (Supplementary Figure S6C). After reacting with glutaraldehyde (GA) in LPS-stimulated macrophages, the majority of endogenous CNBP was detected at the predicted dimer size in reducing gel conditions (Figure 6F). To confirm these results, we used HEK 293T cells expressing GFP-CNBP and Myc-CNBP. Consistent with the previous results, CNBP clearly underwent dimerization (Figure 6G). Similar to the results seen with CNBP phosphorylation, no significant inhibition of dimerization was observed with single-point mutants ($CNBP^{T173A}$ or $CNBP^{T177A}$) (Supplementary Figure S6C). Interestingly, CNBP dimerization was strongly dependent on its phosphorylation at Thr^{173} and Thr^{177}, as the dimerization of $CNBP^{T173/177A}$ was impaired in response to LPS (Figure 6H). Altogether, we conclude that the phosphorylation of CNBP at Thr^{173}/Thr^{177} is critical for its dimerization, which subsequently induces nuclear translocation and immune response activation.

CNBP depletion-mediated reduced IL-6 production causes defects of bacterial defense

Next, we validated the ability of CNBP to induce cytokine production in response to LPS stimulation. Similar to our previous data, this depletion impaired the LPS-induced production of IL-6, but not TNF-α, in RAW macrophages, BMDCs and BMDMs (Figure 7A). Additional shRNA (shRNA #2)-expressing macrophages consistently showed a severe reduction of IL-6 production when compared with control cells (Figure 7B). To examine whether TLR-agonist specificity is involved in CNBP-mediated cytokine production, we assessed IL-6 production in macrophages that were exposed to CpG-DNA, which activates the TLR9 signaling cascade (40). In *cnbp*-depleted macrophages, the production of IL-6, but not TNF-α, was attenuated in response to CpG-DNA (Figure 7C). Additionally, *cnbp*-overexpressing macrophages showed a significant increase in the level of IL-6, but not TNF-α (Figure 7D). To confirm the effects of LPS-induced CNBP function in a bacterial infection system, we examined *il-1b*, *il-6*, *il-12b*, *il-15*, *ccl3*, *ccl4*, *ccl5* and *ccl9* gene expression in MEFs infected by *Shigella flexneri* (M90T), a Gram-negative bacterium that robustly induces inflammatory cytokine gene expression (41). Consistent with all the LPS-related dataset, expression of all tested genes was impaired in *Shigella*-infected *cnbp*-depleted cells (Figure 7E; see also Supplementary Figure S7). We also assessed gene expression levels of these sustained cytokines in MEFs infected by a non-invasive derivative of M90T (BS176). Compared with the M90T results, only very small amounts of cytokine mRNA were observed in BS176-infected and *cnbp*-depleted cells (Figure 7E).

Depletion of CNBP leads to an increased susceptibility to bacterial infection *in vivo*

To determine the effect of CNBP-mediated IL-6 on the immune system *in vivo*, we examined its physiological role using a zebrafish inflammation model, a powerful model system for studying inflammatory and sepsis responses (42–48). Zebrafish possess only innate immunity until 7 days post-fertilization (dpf) and produce proinflammatory cytokines that are similar to those in rodents and humans (46). In addition, many key components of the TLR signaling pathway are ubiquitously expressed in zebrafish (49). We designed zebrafish *cnbp*-targeted morpholino oligos (MO#1

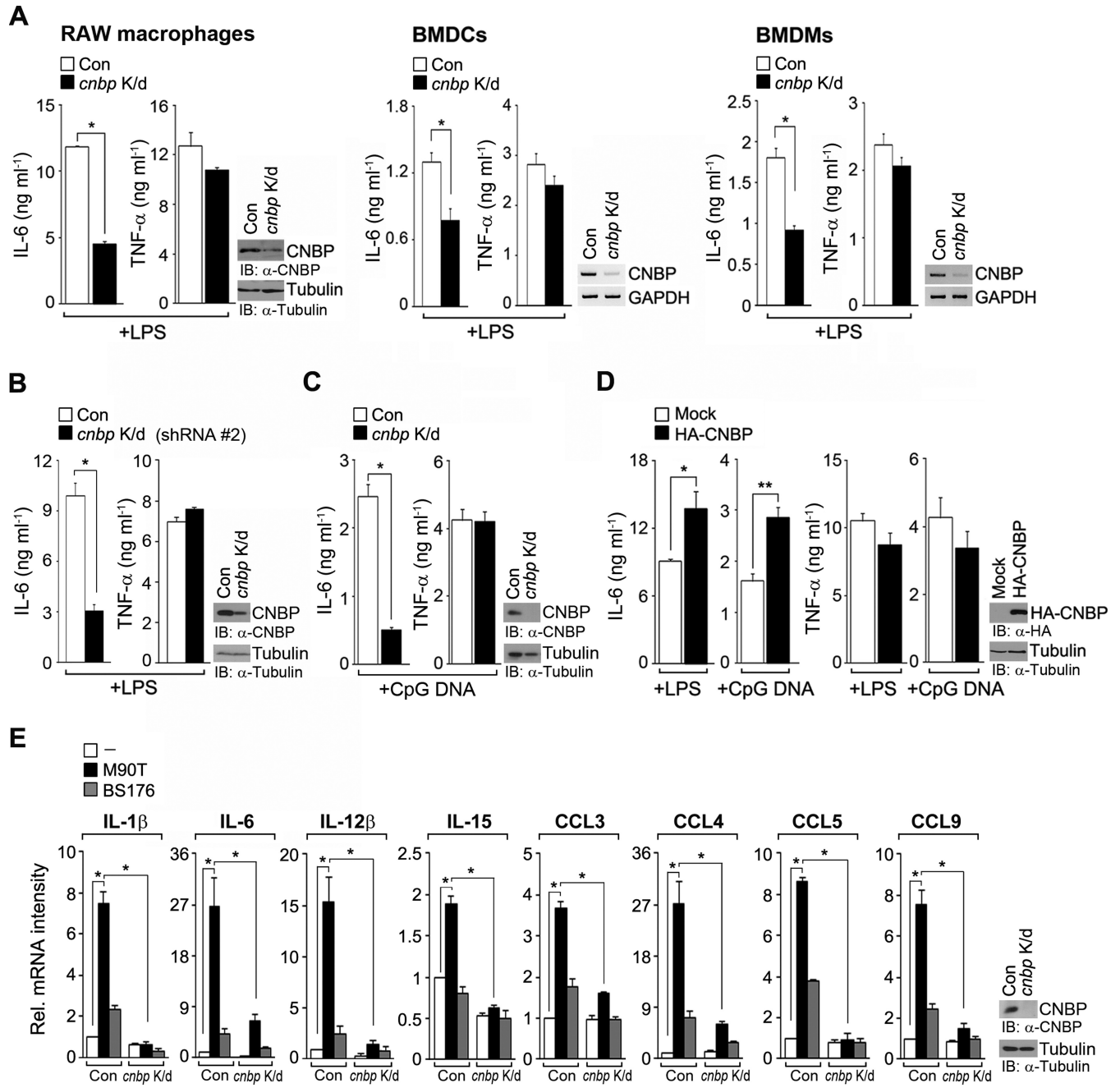

Figure 7. CNBP depletion impairs IL-6 production, causing defects of bacterial defense. (**A**–**D**) CNBP expression affects the LPS (80 ng ml^{-1})- or CpG-DNA (1 μM)-induced production of IL-6, but not TNF-α. ELISA of IL-6 and TNF-α expression in culture supernatants of CNBP-depleted or -overexpressed RAW macrophages, BMDCs or BMDMs. *$P < 0.05$ and **$P < 0.01$ (Student's *t*-test). (**E**) CNBP depletion impairs mRNA expression of sustained inflammatory cytokines after bacterial infection. MEFs were transduced with retrovirus expressing either GFP shRNA or CNBP shRNA, and then cells were infected with *Shigella flexneri* for 1 h. The mRNA expression level of indicated genes was performed by RT-PCR. Band intensity from RT-PCR results was quantified using densitometry, and results were normalized to *gapdh*. *$P < 0.01$ (Student's *t*-test). Immunoblot or RT-PCR analysis of transduction efficiency (right panels of A–E). Data are representative of at least two independent experiments and are presented as mean ± s.d. in A–E.

and MO#2) and injected them into the fertilized embryos (Supplementary Figure S8A). The concentrations of MOs for injection were decided according to a previous report demonstrating no off-target and/or toxicological effects (50). We found that the *cnbp* MOs efficiently reduced *cnbp* expression by producing alternatively spliced forms of *cnbp* in the MO-injected embryos (morphants) (Supplementary Figure S8B). In comparison with the controls, *cnbp* morphants exhibited morphological abnormalities such as a small brain, heart edema and curved tail that did not affect the morphants' survival for at least one week (Supplementary Figure S8C). To examine *il-6* mRNA expression in *cnbp*-depleted zebrafish under inflammatory conditions, we injected LPS into the yolk of zebrafish larvae at 3 dpf. Con-

sistent with the *in vitro* results, *cnbp* morphants exhibited a significant decrease in *il-6* mRNA levels (Figure 8A).

Next, we examined the recruitment of macrophages and neutrophils to LPS-infected sites because leukocyte infiltration is a characteristic of inflammation. Infiltration of macrophages in *cnbp* morphants was severely defective relative to control morphants (Figure 8B). Furthermore, neutrophil infiltration was also impaired at the LPS-injected sites of *cnbp* morphants (Supplementary Figure S8D). Similar to LPS injection, neutrophil infiltration to the *Shigella*-infected site was severely impaired in *cnbp* morphants (Figure 8C). To ascertain the effect of impaired leukocyte infiltration on the *cnbp*-silenced innate immune response, we compared the survival rates between control and *cnbp* morphants after infections with M90T. We intravenously injected the bacteria at 1×10^3 CFU, an appropriate sublethal dose (47), into zebrafish larvae. The results showed that *cnbp* morphants had decreased survivability 24 h after the infection, whereas control morphants exhibited more than 90% survival (Figure 8D). BS176 infection was little affected the survival rates of *cnbp* morphants. From these results, we hypothesized higher mortality in the *cnbp* morphants might be due to increased bacterial burden resulting from impaired leukocyte infiltration. Therefore, we counted CFU of *Shigella* in control and *cnbp* morphants. We observed a larger number of CFU of M90T, even of BS176, in *cnbp* morphants, suggesting a defect in bacterial clearance by CNBP depletion during inflammation (Figure 8E). Moreover, injecting *cnbp* morphants with wild-type *cnbp* mRNA rescued *il-6* mRNA production during LPS stimulation and highly increased the survivability of *cnbp*-depleted zebrafish after *Shigella* infection, similar to control morphants (Figure 8F and G). Taken altogether, we conclude that CNBP-mediated inflammatory cytokine gene expression is essential for the activation of innate immune signaling during bacterial infections.

DISCUSSION

The central finding of our study is that CNBP performs dual functions to activate transcription of immune response genes in response to LPS stimulation. These functions occur in a time-dependent manner. Specifically, we found that: (i) CNBP binds to specific DNA sequences in the promoters of sustained inflammatory genes, such as *il-1b*, *il-6*, *il-12b*, *il-15*, *ccl3*, *ccl4*, *ccl5*, *ccl7*, *ccl9* and *ccl22*, thus inducing the expression of these genes directly; (ii) NF-κB rapidly activates *cnbp* expression by binding to an NF-κB-binding consensus sequence in the proximal *cnbp* promoter region; (iii) CNBP activates its own expression later in the response to LPS by binding persistently to its own promoter, producing a positive feedback mechanism of autoregulation and robust levels of CNBP induce maximal transcription of *il-6* during a prolonged LPS stimulation; (iv) LPS stimulates the translocation of CNBP into the nucleus by TAK1/PKC/CK1-dependent phosphorylation of Thr^{173} and Thr^{177} and phosphorylation-mediated dimerization; and (v) CNBP deficiency significantly attenuates cytokine production, and *cnbp*-depleted zebrafish are severely susceptible to *Shigella flexneri* infection. Collectively, these observations support a role for CNBP as a critical transcription factor and a key regulator of the prolonged expression of sustained cytokine IL-6 during persistent LPS stimulation or Gram-negative bacterial infection (Supplementary Figure S9).

Our findings provide critical insight into the role of CNBP in the temporal control of immune gene expression to promote appropriate host responses to infection. Autoregulatory feed-forward circuits are used by eukaryotic cells to convert a graded input into a binary response in eukaryotic gene networks. Therefore, positive feedback loops are highly conserved in vertebrate evolution (51–53). Here, we show that LPS signals for translocation of NF-κB to the nucleus, where it rapidly starts to induce expression of *il-6* and *cnbp*. However, because NF-κB is generally involved in a modest increase of *il-6* in the primary response to infections, NF-κB-induced *cnbp* expression is crucial for robust and stable *il-6* expression during persistent LPS stimulation. Moreover, elevated levels of CNBP by NF-κB sequentially activate its own expression by binding to the 5′ regulatory element of its promoter, which subsequently produces high levels of CNBP to promote sustained *il-6* expression. Interestingly, CCAAT/enhancer-binding protein-δ (C/EBPδ) is involved in sensing transient and persistent TLR4-mediated signals in a different manner (26). Thus, there may be a tight correlation between CNBP and C/EBPδ that involves autoinduction and stable expression of sustained cytokines during persistent infections, thereby enabling effective reprogramming of immune cell function and governing distinct functional modules in a transcriptional regulatory network.

Post-translational modification of NF-κB subunits, particularly by phosphorylation, is essential for efficient target gene transcription (54). In particular, the p65 subunit contains 12 phospho-acceptor sites, which can be differentially phosphorylated in a signal-dependent manner. These modifications control NF-κB-mediated transcription by impeding or promoting its association with histone deacetylase-1 (HDAC1) (55,56), altering the binding of key components of the transcriptional machinery (57,58), or regulating p65 stability and nuclear import (59,60). Similarly, CNBP also contains various putative phosphorylation sites including threonine (Thr) residues 173 and 177. As we have shown, CNBP can be phosphorylated by TAK1, PKC and CK1. It is possible that specific kinase-dependent CNBP phosphorylation at different sites may affect its functional activity, subcellular localization and binding networks in transcriptional circuits during infections and various pathological conditions, such as cancers and autoimmune diseases.

As shown previously, *cnbp* expression is very low in the intestine compared to other rat tissues (61). Because the gut interfaces with a dense, long-term, resident microbial community (62), the intestinal immune cell population plays an important role in maintaining immune tolerance through the activation of regulatory T cells and the restriction of TLR signaling (63,64). In particular, patients with inflammatory bowel disease exhibit sustained TLR-driven inflammatory responses, which exacerbate tissue injury and intestinal tumorigenesis (64). Based on our findings, we speculate that the induction of negative transcriptional regulators by intestinal cells may contribute to the low expression level of CNBP in the intestine. This serves to dampen

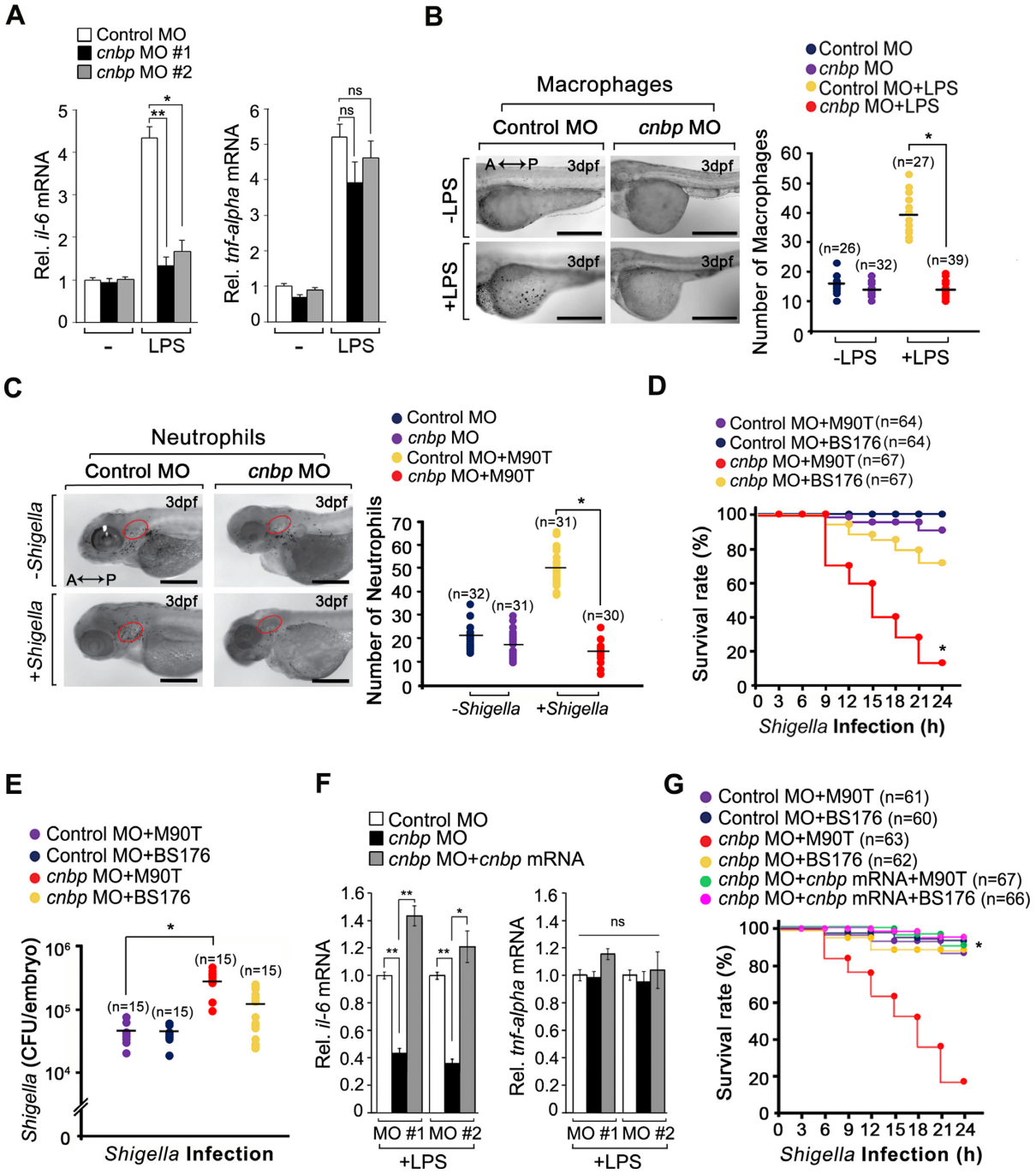

Figure 8. Depletion of CNBP leads to an increased susceptibility to bacterial infection *in vivo*. (**A**) The mRNA levels of *il-6*, but not *tnf-α*, decreased in the *cnbp* morphants. Control and *cnbp* morpholino oligos (MOs) were injected into zebrafish embryos along with LPS (1 mg ml^{-1}) at 24 hpf. Three hours after the infection, *il-6* or *tnf-α* mRNA was measured by RT-qPCR analysis. $*P < 0.01$ and $**P < 0.001$ (Student's *t*-test). (**B**) Macrophages in *cnbp*-depleted zebrafish larvae fail to migrate to the inflammatory foci during LPS infection. To compare the infiltration of macrophages between control and *cnbp* morphants after LPS infection, larvae were collected at 3 h post-infection (hpi) and stained with 2.5 μg ml^{-1} Neutral Red (NR) solution. Migration of NR-stained macrophages was observed under a dissecting microscope. Images were captured and analyzed using a mono-camera and the NIS-Elements software, respectively. Scale bars, 200 μm, $*P < 0.001$ (Student's *t*-test). (**C**) Infiltration of neutrophils was defective in *cnbp* morphants during *Shigella* infection. The *Shigella* M90T was injected into the otic vesicle (circle) of the control and *cnbp* morphants at 3 dpf. The zebrafish larvae were fixed with 4% formaldehyde and permeabilized with ethanol for staining with 0.03% SB at 4 hpi. The migration of SB-stained neutrophils observed by a dissecting microscope was photographed and analyzed using NIS-Elements software. Scale bars, 500 μm. $*P < 0.001$ (Student's *t*-test). (**D**) Survival rates of zebrafish in control or *cnbp* morphants after *Shigella* M90T or BS176 infection. The larvae were injected intravenously with 1×10^3 CFU of *Shigella* at 72 hpf and incubated at 28°C for 24 h. The survival rates of zebrafish larvae were measured during 24 h after the bacteria infection. $*P < 0.01$ (Mantel-Cox log-rank test). (**E**) Bacterial burden in control and *cnbp* morphants after *Shigella* infection with 1×10^3 CFU at 72 hpf and incubation for 24 h. $*P < 0.001$ (Student's *t*-test). (**F** and **G**) The delivery of wild-type *cnbp* mRNA to *cnbp* morphants rescued *il-6* mRNA production and survival during infection. $*P < 0.01$ and $**P < 0.001$ (Student's *t*-test in F or $*P < 0.001$ (Mantel-Cox log-rank test) in G. Data are representative of three independent experiments and are presented as mean ± s.d. in A and F.

any type of sustained inflammation that may be evoked by persistent signals from resident microbiota. Additionally, aberrant CNBP may correlate with inflammatory diseases, which could be characterized by excessive CNBP expression. Thus, our study provides further insight into the molecular pathologies of autoimmune diseases and various cancers, thereby contributing to the development of improved therapeutic strategies for these diseases.

SUPPLEMENTARY DATA

Supplementary Data are available at NAR Online.

ACKNOWLEDGEMENTS

We thank Dr Alxander Hoffmann (University of San Diego, USA), Dr Dong Wook Kim (Department of Pharmacy, Hanyang University, South Korea) and Dr Kwang Chul Chung (Yonsei University, South Korea) for *p65*-deficient MEFs, *Shigella* M90T and BS176 strains, and *nf-kb* luciferase reporter vector, respectively.
Author contributions: E.L., T.A.L., J.H.K., E.A.R., S.K., A.P., H.J.C., H.D.H. and J.L.C conducted experiments and analyzed data. E.L., J.E.L, S.L. and B.P. designed experiments and wrote the manuscript.

FUNDING

Korean Health Technology R&D Project, Ministry of Health & Welfare, Republic of Korea [HI14C2542]; Ministry of Science, ICT, and future planning (National Research Foundation of Korea (NRF), Basic Science Research Program) [2015R1A2A1A15055053, 2015R1D1A1A02062058]; Korean Government (MSIP) (NRF) [NRF-2016R1A5A1010764 to B.P., 2016R1C1B2008930 to J.E.L.]; Ministry of Agriculture, Food, and Rural Affairs (Strategic Initiative for Microbiomes in Agriculture and Food) [916006-2]; Ministry of Education (NRF, Basic Science Research Program) [2015R1D1A1A01060181 to S.L.]; National Cancer Center of Korea [NCC-1710210 to S.L.]; Brain Korea (BK21) PLUS Program (to T.A.L., E.A.R., S.K., A.P., H.J.C., H.D.H., J.L.C.); Korean Government (NRF) [NRF-2013-Global Ph.D. Fellowship Program to H.J.C.]. Funding for open access charge: Wellcome Trust.
Conflict of interest statement. None declared.

REFERENCES

1. Calcaterra,N.B., Armas,P., Weiner,A.M. and Borgognone,M. (2010) CNBP: a multifunctional nucleic acid chaperone involved in cell death and proliferation control. *IUBMB Life*, **62**, 707–714.
2. Pellizzoni,L., Lotti,F., Rutjes,S.A. and Pierandrei-Amaldi,P. (1998) Involvement of the Xenopus laevis Ro60 autoantigen in the alternative interaction of La and CNBP proteins with the 5′UTR of L4 ribosomal protein mRNA. *J. Mol. Biol.*, **281**, 593–608.
3. Michelotti,E.F., Tomonaga,T., Krutzsch,H. and Levens,D. (1995) Cellular nucleic acid binding protein regulates the CT element of the human c-myc protooncogene. *J. Biol. Chem.*, **270**, 9494–9499.
4. Chen,W., Wang,Y., Abe,Y., Cheney,L., Udd,B. and Li,Y.P. (2007) Haploinsuffciency for Znf9 in Znf9+/- mice is associated with multiorgan abnormalities resembling myotonic dystrophy. *J. Mol. Biol.*, **368**, 8–17.
5. Flink,I.L. and Morkin,E. (1995) Alternatively processed isoforms of cellular nucleic acid-binding protein interact with a suppressor region of the human beta-myosin heavy chain gene. *J. Biol. Chem.*, **270**, 6959–6965.
6. Margarit,E., Armas,P., Garcia Siburu,N. and Calcaterra,N.B. (2014) CNBP modulates the transcription of Wnt signaling pathway components. *Biochim. Biophys. Acta*, **1839**, 1151–1160.
7. Liquori,C.L., Ricker,K., Moseley,M.L., Jacobsen,J.F., Kress,W., Naylor,S.L., Day,J.W. and Ranum,L.P. (2001) Myotonic dystrophy type 2 caused by a CCTG expansion in intron 1 of ZNF9. *Science*, **293**, 864–867.
8. Niedowicz,D.M., Beckett,T.L., Holler,C.J., Weidner,A.M. and Murphy,M.P. (2010) APP(DeltaNL695) expression in murine tissue downregulates CNBP expression. *Neurosci. Lett.*, **482**, 57–61.
9. Covey,S.N. (1986) Amino acid sequence homology in gag region of reverse transcribing elements and the coat protein gene of cauliflower mosaic virus. *Nucleic Acids Res.*, **14**, 623–633.
10. Warden,C.H., Krisans,S.K., Purcell-Huynh,D., Leete,L.M., Daluiski,A., Diep,A., Taylor,B.A. and Lusis,A.J. (1994) Mouse cellular nucleic acid binding proteins: a highly conserved family identified by genetic mapping and sequencing. *Genomics*, **24**, 14–19.
11. Yasuda,J., Mashiyama,S., Makino,R., Ohyama,S., Sekiya,T. and Hayashi,K. (1995) Cloning and characterization of rat cellular nucleic acid binding protein (CNBP) cDNA. *DNA Res.*, **2**, 45–49.
12. van Heumen,W.R., Claxton,C. and Pickles,J.O. (1997) Sequence and tissue distribution of chicken cellular nucleic acid binding protein cDNA. *Comp. Biochem. Physiol. B Biochem. Mol. Biol.*, **118**, 659–665.
13. Shimizu,K., Chen,W., Ashique,A.M., Moroi,R. and Li,Y.P. (2003) Molecular cloning, developmental expression, promoter analysis and functional characterization of the mouse CNBP gene. *Gene*, **307**, 51–62.
14. Armas,P., Cabada,M.O. and Calcaterra,N.B. (2001) Primary structure and developmental expression of Bufo arenarum cellular nucleic acid-binding protein: changes in subcellular localization during early embryogenesis. *Dev. Growth Differ.*, **43**, 13–23.
15. Tieleman,A.A., den Broeder,A.A., van de Logt,A.E. and van Engelen,B.G. (2009) Strong association between myotonic dystrophy type 2 and autoimmune diseases. *J. Neurol. Neurosurg. Psychiatry*, **80**, 1293–1295.
16. Meyer,A., Lannes,B., Carapito,R., Bahram,S., Echaniz-Laguna,A., Geny,B., Sibilia,J. and Gottenberg,J.E. (2015) Eosinophilic myositis as first manifestation in a patient with type 2 myotonic dystrophy CCTG expansion mutation and rheumatoid arthritis. *Neuromuscul. Disord.*, **25**, 149–152.
17. Rhodes,J.D., Lott,M.C., Russell,S.L., Moulton,V., Sanderson,J., Wormstone,I.M. and Broadway,D.C. (2012) Activation of the innate immune response and interferon signalling in myotonic dystrophy type 1 and type 2 cataracts. *Hum. Mol. Genet.*, **21**, 852–862.
18. Askanas,V. and Engel,W.K. (2007) Inclusion-body myositis, a multifactorial muscle disease associated with aging: current concepts of pathogenesis. *Curr. Opin. Rheumatol.*, **19**, 550–559.
19. Querfurth,H.W., Suhara,T., Rosen,K.M., McPhie,D.L., Fujio,Y., Tejada,G., Neve,R.L., Adelman,L.S. and Walsh,K. (2001) Beta-amyloid peptide expression is sufficient for myotube death: implications for human inclusion body myopathy. *Mol. Cell Neurosci.*, **17**, 793–810.
20. Gordon,S. (2003) Alternative activation of macrophages. *Nat. Rev. Immunol.*, **3**, 23–35.
21. Taylor,P.R., Martinez-Pomares,L., Stacey,M., Lin,H.H., Brown,G.D. and Gordon,S. (2005) Macrophage receptors and immune recognition. *Annu. Rev. Immunol.*, **23**, 901–944.
22. Medzhitov,R. and Horng,T. (2009) Transcriptional control of the inflammatory response. *Nat. Rev. Immunol.*, **9**, 692–703.
23. Anderson,P. (2008) Post-transcriptional control of cytokine production. *Nat. Immunol.*, **9**, 353–359.
24. Beutler,B. (2000) Tlr4: central component of the sole mammalian LPS sensor. *Curr. Opin. Immunol.*, **12**, 20–26.
25. Shalek,A.K., Satija,R., Shuga,J., Trombetta,J.J., Gennert,D., Lu,D., Chen,P., Gertner,R.S., Gaublomme,J.T., Yosef,N. *et al.* (2014) Single-cell RNA-seq reveals dynamic paracrine control of cellular variation. *Nature*, **510**, 363–369.
26. Litvak,V., Ramsey,S.A., Rust,A.G., Zak,D.E., Kennedy,K.A., Lampano,A.E., Nykter,M., Shmulevich,I. and Aderem,A. (2009) Function of C/EBPdelta in a regulatory circuit that discriminates

between transient and persistent TLR4-induced signals. *Nat. Immunol.*, **10**, 437–443.
27. Ramsey,S.A., Klemm,S.L., Zak,D.E., Kennedy,K.A., Thorsson,V., Li,B., Gilchrist,M., Gold,E.S., Johnson,C.D., Litvak,V. *et al.* (2008) Uncovering a macrophage transcriptional program by integrating evidence from motif scanning and expression dynamics. *PLoS Comput. Biol.*, **4**, e1000021.
28. Ravasi,T., Wells,C.A. and Hume,D.A. (2007) Systems biology of transcription control in macrophages. *Bioessays*, **29**, 1215–1226.
29. Stormo,G.D. and Zhao,Y. (2010) Determining the specificity of protein-DNA interactions. *Nat. Rev. Genet.*, **11**, 751–760.
30. Armas,P., Nasif,S. and Calcaterra,N.B. (2008) Cellular nucleic acid binding protein binds G-rich single-stranded nucleic acids and may function as a nucleic acid chaperone. *J. Cell Biochem.*, **103**, 1013–1036.
31. Armas,P., Margarit,E., Mouguelar,V.S., Allende,M.L. and Calcaterra,N.B. (2013) Beyond the binding site: in vivo identification of tbx2, smarca5 and wnt5b as molecular targets of CNBP during embryonic development. *PLoS One*, **8**, e63234.
32. Bailey,T.L., Williams,N., Misleh,C. and Li,W.W. (2006) MEME: discovering and analyzing DNA and protein sequence motifs. *Nucleic Acids Res.*, **34**, W369–W373.
33. Hayden,M.S. and Ghosh,S. (2008) Shared principles in NF-kappaB signaling. *Cell*, **132**, 344–362.
34. Saitoh,T., Tun-Kyi,A., Ryo,A., Yamamoto,M., Finn,G., Fujita,T., Akira,S., Yamamoto,N., Lu,K.P. and Yamaoka,S. (2006) Negative regulation of interferon-regulatory factor 3-dependent innate antiviral response by the prolyl isomerase Pin1. *Nat. Immunol.*, **7**, 598–605.
35. Lombardo,V.A., Armas,P., Weiner,A.M. and Calcaterra,N.B. (2007) In vitro embryonic developmental phosphorylation of the cellular nucleic acid binding protein by cAMP-dependent protein kinase, and its relevance for biochemical activities. *FEBS J.*, **274**, 485–497.
36. Zhong,H., Voll,R.E. and Ghosh,S. (1998) Phosphorylation of NF-kappa B p65 by PKA stimulates transcriptional activity by promoting a novel bivalent interaction with the coactivator CBP/p300. *Mol. Cell*, **1**, 661–671.
37. Wang,Y., Hu,L., Tong,X. and Ye,X. (2014) Casein kinase 1gamma1 inhibits the RIG-I/TLR signaling pathway through phosphorylating p65 and promoting its degradation. *J. Immunol.*, **192**, 1855–1861.
38. Oeckinghaus,A., Hayden,M.S. and Ghosh,S. (2011) Crosstalk in NF-kappaB signaling pathways. *Nat. Immunol.*, **12**, 695–708.
39. Lin,R., Heylbroeck,C., Pitha,P.M. and Hiscott,J. (1998) Virus-dependent phosphorylation of the IRF-3 transcription factor regulates nuclear translocation, transactivation potential, and proteasome-mediated degradation. *Mol. Cell. Biol.*, **18**, 2986–2996.
40. Latz,E., Schoenemeyer,A., Visintin,A., Fitzgerald,K.A., Monks,B.G., Knetter,C.F., Lien,E., Nilsen,N.J., Espevik,T. and Golenbock,D.T. (2004) TLR9 signals after translocating from the ER to CpG DNA in the lysosome. *Nat. Immunol.*, **5**, 190–198.
41. Ogawa,M., Handa,Y., Ashida,H., Suzuki,M. and Sasakawa,C. (2008) The versatility of Shigella effectors. *Nat. Rev. Microbiol.*, **6**, 11–16.
42. Davis,J.M., Clay,H., Lewis,J.L., Ghori,N., Herbomel,P. and Ramakrishnan,L. (2002) Real-time visualization of mycobacterium-macrophage interactions leading to initiation of granuloma formation in zebrafish embryos. *Immunity*, **17**, 693–702.
43. Dios,S., Balseiro,P., Costa,M.M., Romero,A., Boltana,S., Roher,N., Mackenzie,S., Figueras,A. and Novoa,B. (2014) The involvement of cholesterol in sepsis and tolerance to lipopolysaccharide highlighted by the transcriptome analysis of zebrafish (Danio rerio). *Zebrafish*, **11**, 421–433.
44. Mathias,J.R., Perrin,B.J., Liu,T.X., Kanki,J., Look,A.T. and Huttenlocher,A. (2006) Resolution of inflammation by retrograde chemotaxis of neutrophils in transgenic zebrafish. *J. Leukoc. Biol.*, **80**, 1281–1288.
45. Yoo,S.K. and Huttenlocher,A. (2011) Spatiotemporal photolabeling of neutrophil trafficking during inflammation in live zebrafish. *J. Leukoc. Biol.*, **89**, 661–667.
46. Lam,S.H., Chua,H.L., Gong,Z., Lam,T.J. and Sin,Y.M. (2004) Development and maturation of the immune system in zebrafish, Danio rerio: a gene expression profiling, in situ hybridization and immunological study. *Dev. Comp. Immunol.*, **28**, 9–28.
47. Lieschke,G.J. and Currie,P.D. (2007) Animal models of human disease: zebrafish swim into view. *Nat. Rev. Genet.*, **8**, 353–367.
48. Novoa,B., Bowman,T.V., Zon,L. and Figueras,A. (2009) LPS response and tolerance in the zebrafish (Danio rerio). *Fish Shellfish Immunol.*, **26**, 326–331.
49. Purcell,M.K., Smith,K.D., Hood,L., Winton,J.R. and Roach,J.C. (2006) Conservation of toll-like receptor signaling pathways in teleost fish. *Comp. Biochem. Physiol. Part D Genomics Proteomics*, **1**, 77–88.
50. Weiner,A.M., Sdrigotti,M.A., Kelsh,R.N. and Calcaterra,N.B. (2011) Deciphering the cellular and molecular roles of cellular nucleic acid binding protein during cranial neural crest development. *Dev. Growth Differ.*, **53**, 934–947.
51. Becskei,A., Seraphin,B. and Serrano,L. (2001) Positive feedback in eukaryotic gene networks: cell differentiation by graded to binary response conversion. *EMBO J.*, **20**, 2528–2535.
52. Siciliano,V., Menolascina,F., Marucci,L., Fracassi,C., Garzilli,I., Moretti,M.N. and di Bernardo,D. (2011) Construction and modelling of an inducible positive feedback loop stably integrated in a mammalian cell-line. *PLoS Comput. Biol.*, **7**, e1002074.
53. Kielbasa,S.M. and Vingron,M. (2008) Transcriptional autoregulatory loops are highly conserved in vertebrate evolution. *PLoS One*, **3**, e3210.
54. Huang,B., Yang,X.D., Lamb,A. and Chen,L.F. (2010) Posttranslational modifications of NF-kappaB: another layer of regulation for NF-kappaB signaling pathway. *Cell Signal.*, **22**, 1282–1290.
55. Rocha,S., Garrett,M.D., Campbell,K.J., Schumm,K. and Perkins,N.D. (2005) Regulation of NF-kappaB and p53 through activation of ATR and Chk1 by the ARF tumour suppressor. *EMBO J.*, **24**, 1157–1169.
56. Sabatel,H., Di Valentin,E., Gloire,G., Dequiedt,F., Piette,J. and Habraken,Y. (2012) Phosphorylation of p65(RelA) on Ser(547) by ATM represses NF-kappaB-dependent transcription of specific genes after genotoxic stress. *PLoS One*, **7**, e38246.
57. Buss,H., Dorrie,A., Schmitz,M.L., Hoffmann,E., Resch,K. and Kracht,M. (2004) Constitutive and interleukin-1-inducible phosphorylation of p65 NF-{kappa}B at serine 536 is mediated by multiple protein kinases including I{kappa}B kinase (IKK)-{alpha}, IKK{beta}, IKK{epsilon}, TRAF family member-associated (TANK)-binding kinase 1 (TBK1), and an unknown kinase and couples p65 to TATA-binding protein-associated factor II31-mediated interleukin-8 transcription. *J. Biol. Chem.*, **279**, 55633–55643.
58. Wang,D., Westerheide,S.D., Hanson,J.L. and Baldwin,A.S. Jr (2000) Tumor necrosis factor alpha-induced phosphorylation of RelA/p65 on Ser529 is controlled by casein kinase II. *J. Biol. Chem.*, **275**, 32592–32597.
59. Buss,H., Dorrie,A., Schmitz,M.L., Frank,R., Livingstone,M., Resch,K. and Kracht,M. (2004) Phosphorylation of serine 468 by GSK-3beta negatively regulates basal p65 NF-kappaB activity. *J. Biol. Chem.*, **279**, 49571–49574.
60. Drier,E.A., Huang,L.H. and Steward,R. (1999) Nuclear import of the Drosophila Rel protein Dorsal is regulated by phosphorylation. *Genes Dev.*, **13**, 556–568.
61. Rajavashisth,T.B., Taylor,A.K., Andalibi,A., Svenson,K.L. and Lusis,A.J. (1989) Identification of a zinc finger protein that binds to the sterol regulatory element. *Science*, **245**, 640–643.
62. Levine,B. and Kroemer,G. (2008) Autophagy in the pathogenesis of disease. *Cell*, **132**, 27–42.
63. Hooper,L.V. and Macpherson,A.J. (2010) Immune adaptations that maintain homeostasis with the intestinal microbiota. *Nat. Rev. Immunol.*, **10**, 159–169.
64. Maloy,K.J. and Powrie,F. (2011) Intestinal homeostasis and its breakdown in inflammatory bowel disease. *Nature*, **474**, 298–306.